Electronic Supplementary Material (ESI) for Polymer Chemistry.

The push-pull coumarin-based one-component iodonium photoinitiators for cationic nanocomposites 3D-VAT printing.

Filip Petko[1,2], Andrzej Świeży[1,2], Magdalena Jankowska[1], Paweł Stalmach[1], Joanna Ortyl[1,2,3]

[1] Department of Biotechnology and Physical Chemistry, Faculty of Chemical Engineering and Technology, Cracow University of Technology, Warszawska 24, 31-155 Kraków, Poland

[2] Photo HiTech Ltd., Bobrzyńskiego 14, 30-348 Kraków, Poland

[3] Photo4Chem Ltd., Lea 114, 30-133 Kraków, Poland

* Corresponding author: **Joanna Ortyl**

e- mail: jortyl@pk.edu.pl

ORCID iD: 0000-0002-4789-7199

Contents

Section A. Materials and methods

All reagents used in synthesis were purchased from Sigma-Aldrich, Alfa Aesar, Acros Organics and Fluorochem and used without further purification. Silica TLC plates with F-254 nm indicator were purchased from Silicycle Inc. Flash chromatography was performed on Puriflash XS 420, Interchim. ^{1}H NMR and ^{13}C NMR spectra were recorded on Avance III HD 400 MHz Bruker, where chemical shifts were determined with a residual proton of the solvent as standard.

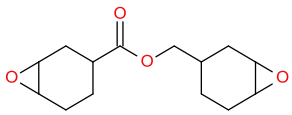

3,4-epoxycyclohexylmethyl 3,4-epoxycyclohexanecarboxylate
CADE

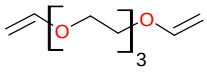

Tri(ethylene glycol)divinyl ether
TEGDVE

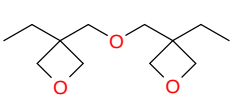

Bis[1-Ethyl(3-oxetanyl)]methyl ether
OXT-221

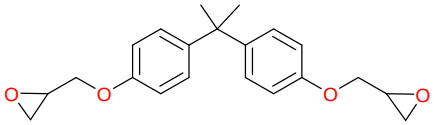

Bisphenol A diglycidyl ether
BADGE

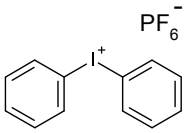

HIP

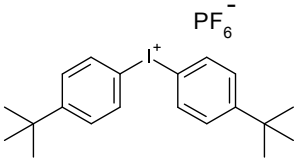

IOD

Figure S1. Structures of monomers and iodonium salts (HIP, IOD) used during photopolymerization and 3D printing experiments.

Section B. Synthetic procedures

Structures of all chromophores are gathered in Figure S2. The synthetic procedures are listed below.

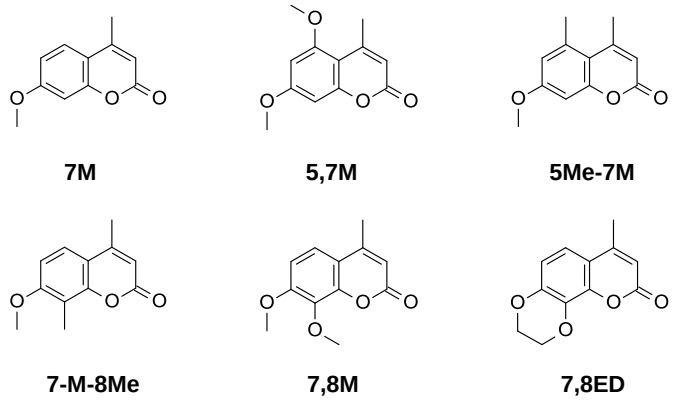

Figure S2. Structures of coumarin chromophores used iodonium salts synthesis.

Synthesis of derivatives of 7-hydroxy-4-methyl-chromen-2-one

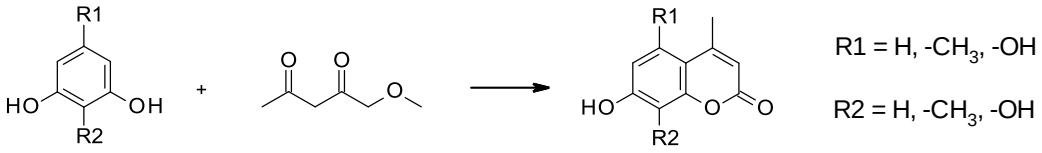

Benzene-1,3-diol (1.0 g, 0.0091 mol) or other diol derivatives was dissolved at 4 ml of acetic acid. Ethyl acetoacetate (1.241 g, 0.0095 mol) was added and the reaction mixture was stirred for 10 min at RT. Sulfuric acid (0.935 g, 0.0095 mol) was slowly added and the reaction mixture was stirred overnight at RT. Next day an excess of water was added. Solid precipitated. It was filtered off**,** washed with water and crystalized from methanol to afford 1.55 g of white powder (Yield = 97 %).

Synthesis of derivatives of 7-methoxy-4-methyl-chromen-2-one

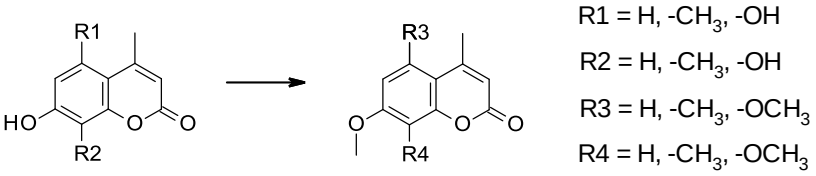

7-hydroxy-4-methyl-chromen-2-one (1.0 g, 0.0057) or other chromen-2-one derivatives was dissolved at 10 ml of acetone. Potassium carbonate (1.374 g, 0.0099 mol) was added and the reaction mixture was stirred for 10 min at reflux. Dimethyl sulfate (1.075 g, 0.0085 mol) was slowly added and the reaction mixture was stirred for 3 h at reflux. The progress of the reaction was controlled with TLC. The reaction mixture was cooled to RT. An excess of water was added. Solid precipitated. It was filtered off, washed with water and crystalized from methanol to afford 0.62 g of white powder (Yield = 57 %).

Synthesis of 7-methyl-2H-[1,4]dioxino [2,3-h] chromen-9(3H)one

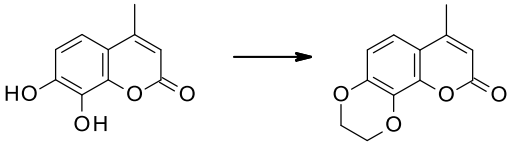

7,8-dihydroxy-4-methyl-chromen-2-one (1.0 g, 0.0052 mol) was dissolved at 5 % solution of NaOH (0.417 g, 0.0104 mol). Benzyltributylammonium chloride (0.032 g, 0.0001 mol) was added and the reaction mixture was stirred overnight at RT. Next day the reaction mixture was warmed to 50 °C. Dibromoethane was added and the reaction mixture was stirred for 5 h at 50 °C. The progress of the reaction was controlled with TLC. An excess of water was added, resulted mixture was extracted with DCM, combined organic layers were washed with water and brine, dried over anhydrous Na_2SO_4, concentrated under vacuum and submitted on flash chromatography (SiO2, hexane/EtOAc 4:1) afforded 0.469 g of product (Yield = 41 %).

Compound	Spectroscopic properties	Yield:
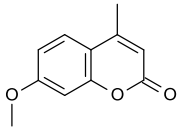 ***7M***	**7-methoxy-4-methylchromen-2-one** ^{1}H NMR (400 MHz, DMSO) δ 7.68 (d, *J* = 8.4 Hz, 1H), 6.96 (m, 2H), 6.20 (d, J = 1.0 Hz, 1H), 3.86 (s, 3H), 2.39 (d, *J* = 1.1 Hz, 3H). ^{13}C NMR (101 MHz, DMSO) δ 162.82, 160.58, 155.23, 153.85, 126.88, 113.55, 112.54, 111.57, 101.15, 56.35, 18.59.	57%
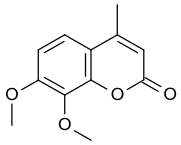 ***7,8M***	**7,8-dimethoxy-4-methyl-chromen-2-one** ^{1}H NMR (400 MHz, DMSO) δ 7.49 (d, *J* = 8.9 Hz, 1H), 7.11 (d, *J* = 9.0 Hz, 1H), 6.23 (d, *J* = 0.9 Hz, 1H), 3.92 (s, 3H), 3.82 (s, 3H), 2.39 (d, *J* = 1.0 Hz, 3H). ^{13}C NMR (101 MHz, DMSO) δ 160.14, 155.57, 154.01, 147.45, 135.70, 120.90, 114.65, 111.90, 109.27, 61.19, 56.80, 18.66.	75%
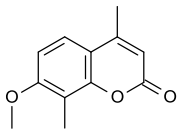 ***7M-8Me***	**7-methoxy-4,8-dimethyl-chromen-2-one** ^{1}H NMR (400 MHz, DMSO) δ 7.60 (d, *J* = 8.8 Hz, 1H), 7.05 (d, *J* = 8.9 Hz, 1H), 6.20 (d, *J* = 1.1 Hz, 1H), 3.91 (s, 3H), 2.39 (d, *J* = 1.1 Hz, 3H), 2.18 (s, 3H). ^{13}C NMR (101 MHz, DMSO) δ 160.62, 160.32, 153.98, 152.35, 124.01, 113.70, 112.65, 111.46, 107.72, 56.61, 18.63, 8.42.	74%
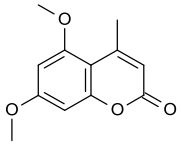 ***5,7M***	**5,7-dimethoxy-4-methyl-chromen-2-one** ^{1}H NMR (400 MHz, DMSO) δ 6.56 (d, *J* = 2.3 Hz, 1H), 6.48 (d, *J* = 2.3 Hz, 1H), 6.00 (d, *J* = 1.0 Hz, 1H), 3.85 (s, 3H), 3.85 (s, 3H), 2.48 (d, *J* = 0.8 Hz, 3H). ^{13}C NMR (101 MHz, DMSO) δ 163.15, 160.12, 159.45, 156.81, 154.61, 111.11, 104.37, 96.04, 94.05, 56.68, 56.33, 24.05.	82%
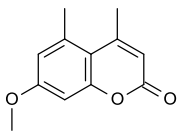 ***5Me-7M***	**7-methoxy-4,5-dimethyl-chromen-2-one** ^{1}H NMR (400 MHz, DMSO) δ 6.78 (s, 1H), 6.11 (d, J = 1.2 Hz, 1H), 3.86 (s, 3H), 2.50 (m, 3H), 2.37 (s, 3H). ^{13}C NMR (101 MHz, DMSO) δ 160.00, 158.13, 155.06, 154.36, 143.69, 113.24, 109.85, 108.51, 107.90, 56.59, 24.12, 21.87.	63%
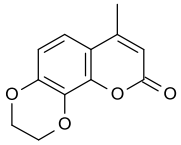 ***7,8ED***	**7-methyl-2H-[1,4]dioxino [2,3-h] chromen-9(3H)one** . ^{1}H NMR (400 MHz, DMSO) δ 7.24 (d, J = 8.7 Hz, 1H), 6.90 (d, J = 8.8 Hz, 1H), 6.23 (d, J=1.1 Hz, 1H), 4.37 (s, 4H), 2.38 (d, J = 1.0 Hz, 3H). ^{13}C NMR (101 MHz, DMSO) δ 160.01, 154.15, 146.68, 143.24, 131.56, 117.04, 114.24, 113.53, 111.84, 64.88, 64.47, 18.74.	41%

Synthesis of new iodonium salts

Synthetic procedures for coumarin based iodonium salts are describe below:

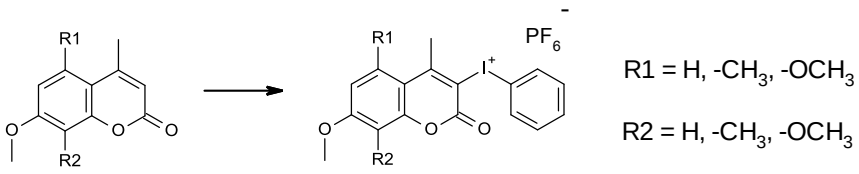

7-methoxy-4-methylchromen-2-one (1.0 g, 0.0053 mol) or other chromen-2-one derivatives was dissolved at glacial acetic acid (7.5 ml). (Diacetoxyiodo)benzene (1.734 g, 0.0054 mol) was added and the reaction mixture was stirred for 15 min h at 50 °C. Sulfuric acid (0.294 ml, 0.0055 mol) was added and the reaction mixture was stirred for 1 h at 50 °C. Potassium hexafluorophosphate (1.065 g, 0.0058 mol) was added and the reaction mixture was stirred for 15 min at 50 °C. The progress of the reaction was controlled with TLC. Acetic anhydride (4.3 ml) was added and the reaction mixture for another 15 min at 50 °C. The reaction mixture was cooled to RT. An excess of water was added. The reaction mixture were stirred for 30 min at RT. Solid precipitated. It was filtered off, washed with water to afford 1.98 g of white powder (Yield = 70 %).

If no solids precipitaded after adding water, the final product was extracted with mixture of DCM and acetone (1:1), combined organic phases were combined, washed with water and dried over Na_2SO_4. Product was purified on flash chromatography (SiO_2, DCM/MeOH 10:1).

Synthesis of new salt based on 7-methyl-2H-[1,4]dioxino [2,3-h] chromen-9(3H)one

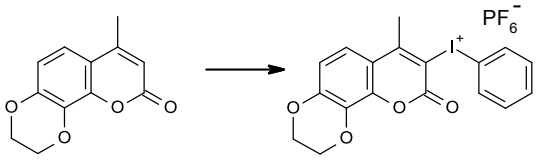

(Diacetoxyiodo)benzene (1.55 g, 0.0048 mol) and p-Toluenesulfonic acid monohydrate (1.066 g, 0.050 mol) were dissolved acetic acid (15 ml) and the reaction mixture was stirred for 15 min at RT. White precipitate was observed. The acetic acid (15 ml) was added to the reaction mixture followed by addition of 7-methyl-2H-[1,4]dioxino [2,3-h] chromen-9(3H)one (1.0 g, 0,0046 mol).The reaction mixture was stirred overnight at RT. An excess of water was added to the reaction mixture. Solid precipitated. It was filtered off, washed with water and dried under vacuum (50 °C) to afford 1.019 of tosyl salt which was used at the next step.

Tosyl salt (1.0 g, 0.0017 mol) was suspended at the acetone (24 ml) and DCM (20 ml) mixture. The potassium hexafluorophosphate (0.342 g, 0.0019 mol) was added and the reaction mixture was stirred for 1 h at RT. An excess of water was added. Phases was separated. Organic phase was washed with water and dried over Na_2SO_4. The product was concentrated to dryness to afford 0.516 g of yellow powder (combined yield of both stages: 42 %).

Obtained new iodonium salts:

Compound	Spectroscopic properties	Yield:
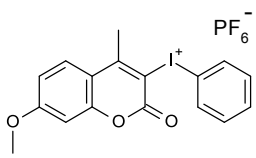 ***7M-P***	**7-methoxy-4-methylchromen-2-one iodonium hexafluorophosphate** ^{1}H NMR (400 MHz, DMSO) δ 8.18 (d, J = 0.8 Hz, 1H), 8.14 (d, J = 1.0 Hz, 1H), 8.02 (d, J = 8.8 Hz, 1H), 7.68 (t, J = 7,4 Hz, 1H), 7.54 (t, J = 7.8 Hz, 2H), 7.13 (d, J = 7.5 Hz, 1H), 7.11 (dd, J = 9.0, 2.5 Hz, 1H), 3.91 (s, 3H), 2.99 (s, 3H). ^{13}C NMR (101 MHz, DMSO) δ 165.45, 163.11, 157.31, 155.63, 135.72, 132.61, 132.20, 129.85, 116.34, 114.29, 112.06, 108.79, 101.36, 56.93, 24.30. MS (ESI) m/z(%): 393 (M^+, 100%) Purity (LC): 97%	70%
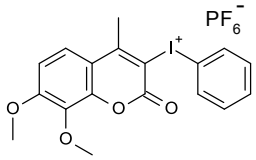 ***7,8M-P***	**7,8-dimethoxy-4-methyl-chromen-2-one iodonium hexafluorophosphate** ^{1}H NMR (400 MHz, DMSO) δ 8.18 (d, J = 1.0 Hz, 1H), 8.16 (d, *J* = 1.1 Hz, 1H), 7.84 (d, *J* = 9.2 Hz, 1H), 7.68 (t, *J* = 7.5 Hz, 1H), 7.54 (t, *J* = 7.8 Hz, 2H), 7.25 (d, *J* = 9.3 Hz, 1H), 3.98 (s, 3H), 3.81 (s, 3H), 2.98 (s, 3H). ^{13}C NMR (101 MHz, DMSO) δ 163.22, 158.12, 156.95, 147.59, 135.80, 135.59, 132.64, 132.21, 124.16, 116.31, 113.02, 110.73, 109.33, 98.01, 61.40, 57.26, 24.42. MS (ESI) m/z(%): 423 (M^+, 100%) Purity (LC): 95%	47%
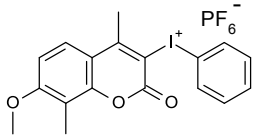 ***7M-8Me-P***	**7-methoxy-4,8-dimethyl-chromen-2-one iodonium hexafluorophosphate** ^{1}H NMR (400 MHz, DMSO) δ 8.17 (d, *J* = 1.0 Hz, 1H), 8.16 (d, *J* = 1.0 Hz, 1H), 7.96 (d, *J* = 9.1 Hz, 1H), 7.68 (t, *J* = 7.4 Hz, 1H), 7.53 (t, *J* = 7.8 Hz, 2H), 7.19 (d, *J* = 9.2 Hz, 1H), 3.96 (s, 3H), 3.00 (s, 3H), 2.17 (s, 3H). ^{13}C NMR (101 MHz, DMSO) δ 163.20, 162.92, 157.33, 152.44, 137.56, 135.71, 132.59, 132.19, 131.12, 127.41, 116.40, 113.16, 112.23, 109.34, 108.89, 57.13, 24.32, 8.41. MS (ESI) m/z(%): 407 (M^+, 100%) Purity (LC): 100%	61%
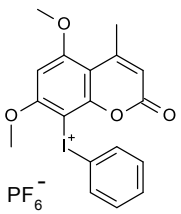 ***5,7M-P***	**5,7-dimethoxy-4-methyl-chromen-2-one iodonium hexafluorophosphate** ^{1}H NMR (400 MHz, DMSO) δ 8.04 (d, *J* = 0.8 Hz, 1H), 8.02 (d, *J* = 1.1 Hz, 1H), 7.63 (t, *J* = 7.4 Hz, 1H), 7.49 (t, *J* = 7.8 Hz, 2H), 6.82 (s, 1H), 6.22 (d, *J* = 1.2 Hz, 1H), 4.10 (d, *J* = 4.9 Hz, 3H), 4.02 (s, 3H), 2.51 (m, 3H). ^{13}C NMR (101 MHz, DMSO) δ 164.04, 161.13, 158.51, 155.14, 154.47, 135.18, 132.39, 132.23, 116.85, 112.14, 105.25, 93.67, 87.23, 58.46, 57.65, 24.02. MS (ESI) m/z(%): 423 (M^+, 100%) Purity (LC): 95%	91%
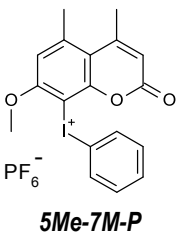 ***5Me-7M-P***	**7-methoxy-4,5-dimethyl-chromen-2-one iodonium hexafluorophosphate** ^{1}H NMR (400 MHz, DMSO) δ 8.13 (d, J = 0.9 Hz 1H), 8.11 (d, *J* = 1.0 Hz, 1H), 7.65 (t, *J* = 7.4 Hz, 1H), 7.51 (t, *J* = 7.8 Hz, 2H), 7.23 (s, 1H), 6.35 (d, *J* = 1.1 Hz, 1H), 3.96 (s, 3H), 2.76 (s, 3H), 2.54 (d, *J* = 0.9 Hz, 3H). ^{13}C NMR (101 MHz, DMSO) δ 161.51, 158.27, 154.90, 153.13, 147.24, 135.37, 132.52, 132.31, 116.48, 114.23, 110.44, 109.21, 100.98, 57.45, 26.2, 24.01.	72%

	MS (ESI) m/z(%): 407 (M^+, 100%) Purity (LC): 99.5%	
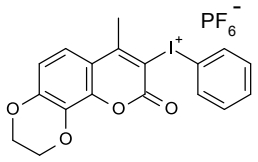 ***7,8ED-P***	**7-methyl-2H-[1,4]dioxino [2,3-h] chromen-9(3H)one iodonium hexafluorophosphate** ^{1}H NMR (400 MHz, DMSO) δ 8.17 (d, *J* = 0.9 Hz, 1H), 8.15 (d, *J* = 1.1 Hz, 1H), 7.68 (tt, *J* = 7.4, 1.3 Hz, 1H), 7.59 (m, 3H), 7.04 (d, *J* = 9.0 Hz, 1H), 4.40 (m, 4H), 2.97 (s, 3H). ^{13}C NMR (101 MHz, DMSO) δ 163.32, 156.77, 149.37, 143.41, 137.57, 135.69, 132.59, 132.19, 131.57, 131.13, 120.04, 116.40, 115.07, 112.74, 109.44, 65.30, 64.51, 24.48. MS (ESI) m/z(%): 421 (M^+, 100%) Purity (LC): 100%	54%

1. ^{1}H NMR spectra of iodonium salts compounds

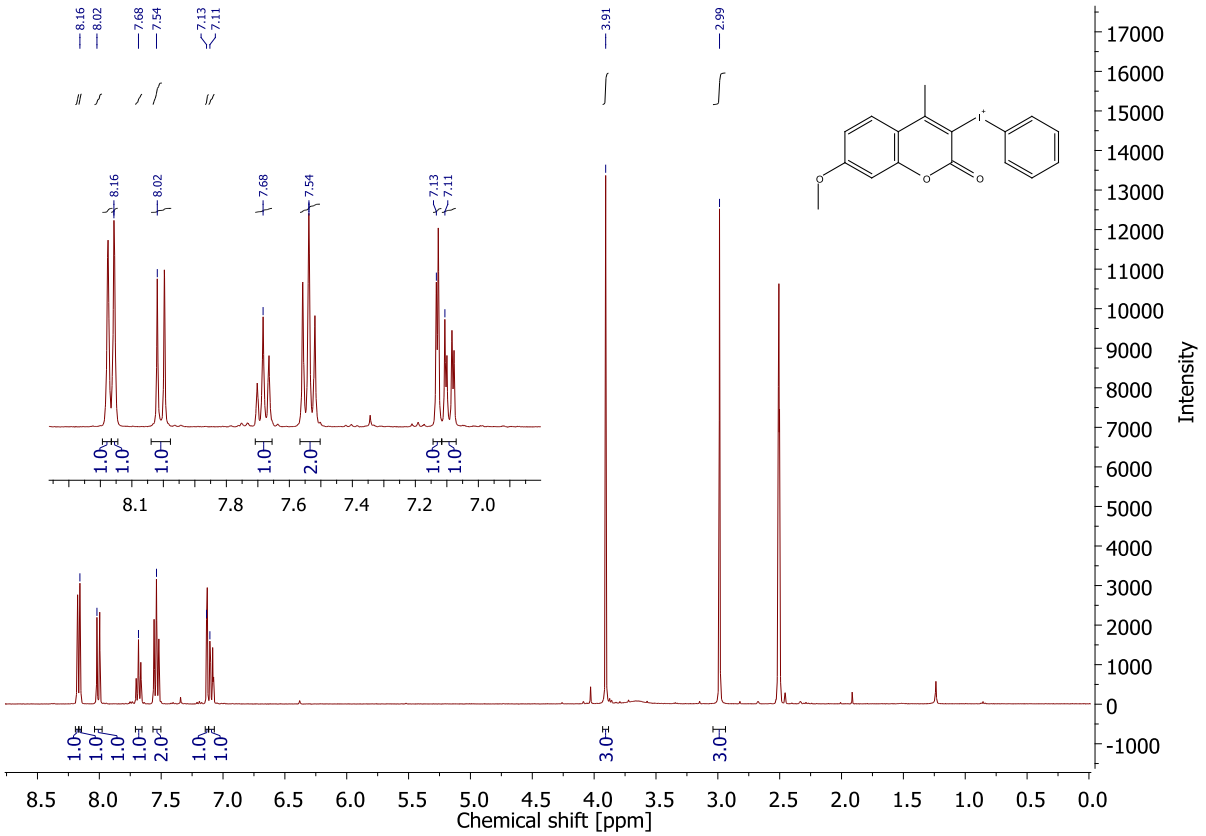

Figure S3: ^{1}H NMR of ***7M-P.***

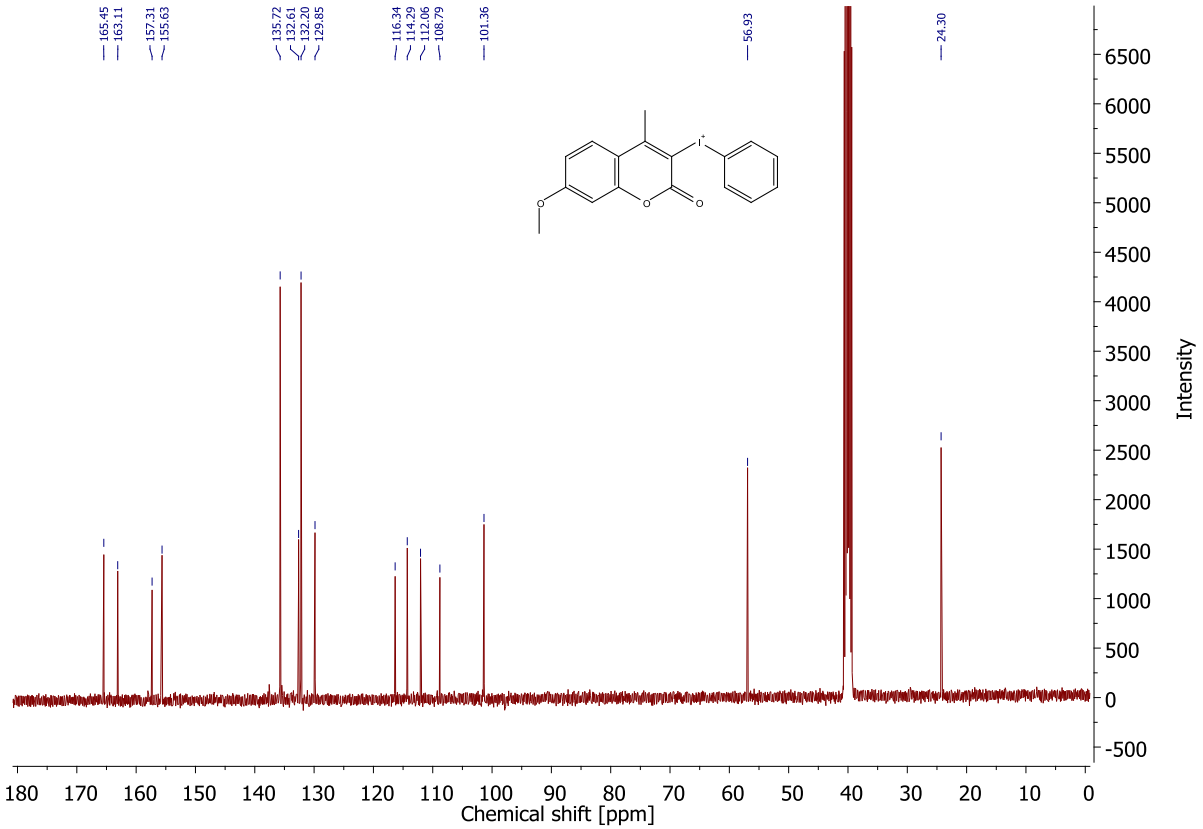

Figure S4: ^{13}C NMR of ***7M-P.***

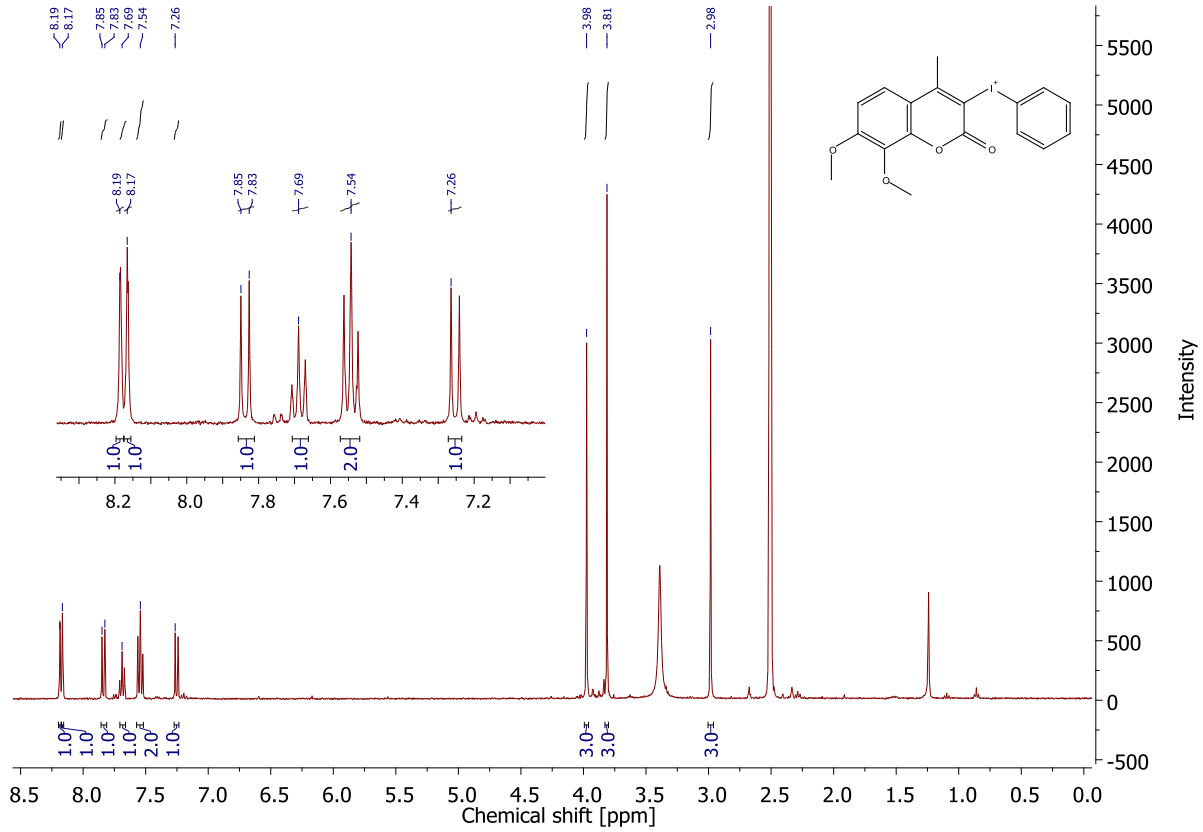

Figure S5: ^{1}H NMR of ***7,8M-P.***

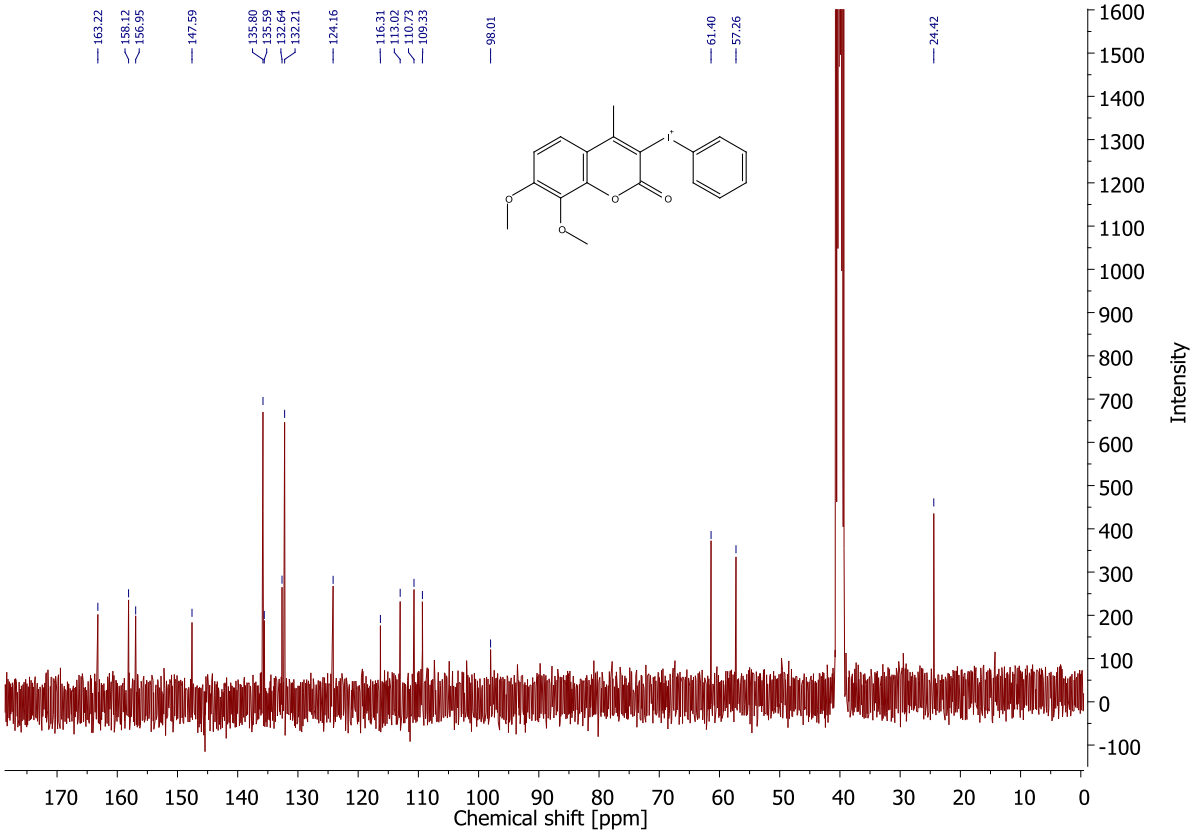

Figure S6: ^{13}C NMR of ***7,8M-P.***

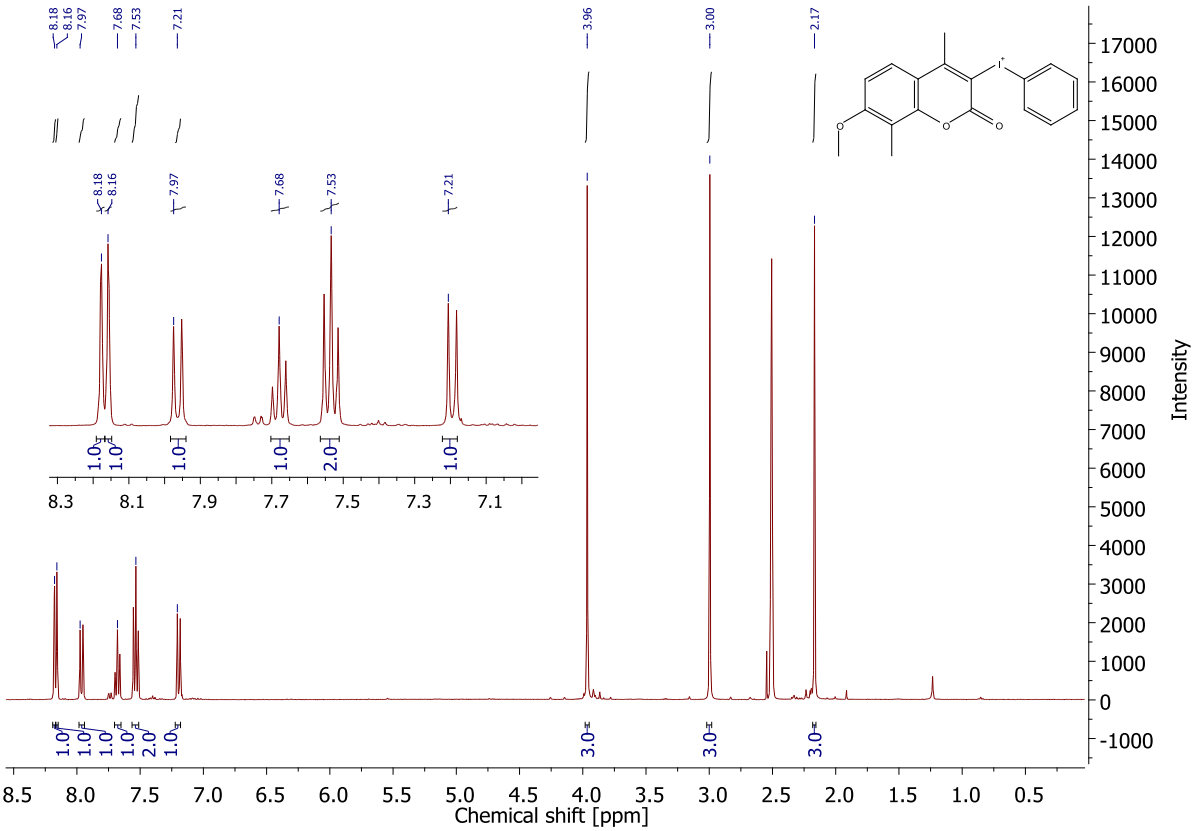

Figure S7: ^{1}H NMR of ***7M-8Me-P.***

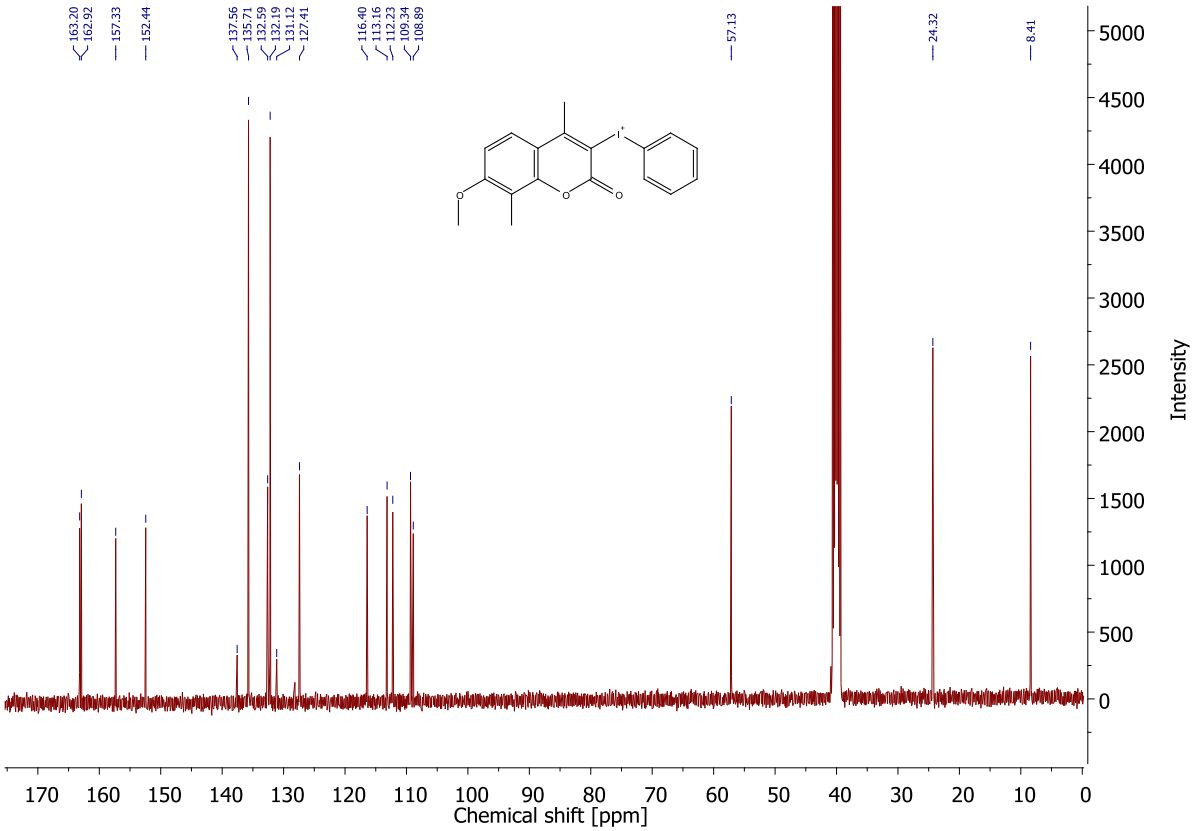

Figure S8: ^{13}C NMR of ***7M-8Me-P.***

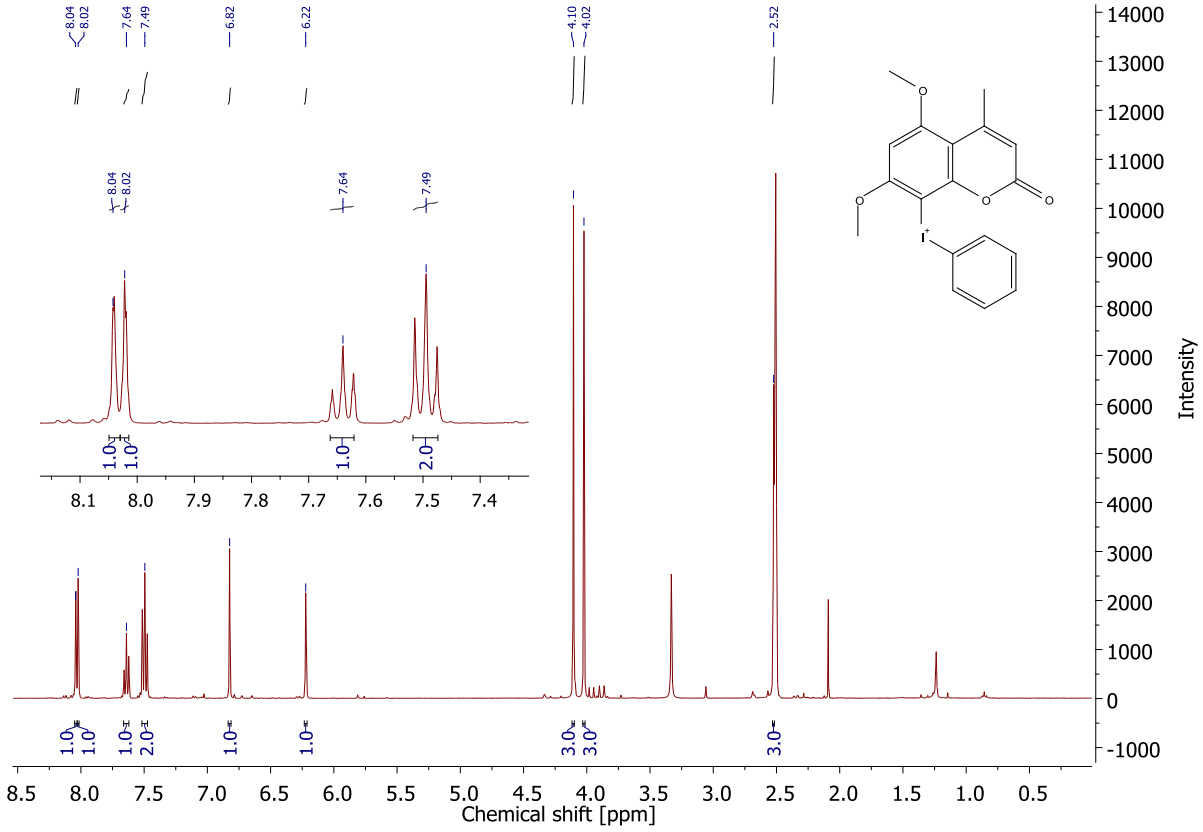

Figure S9: ^{1}H NMR of ***5,7M-P.***

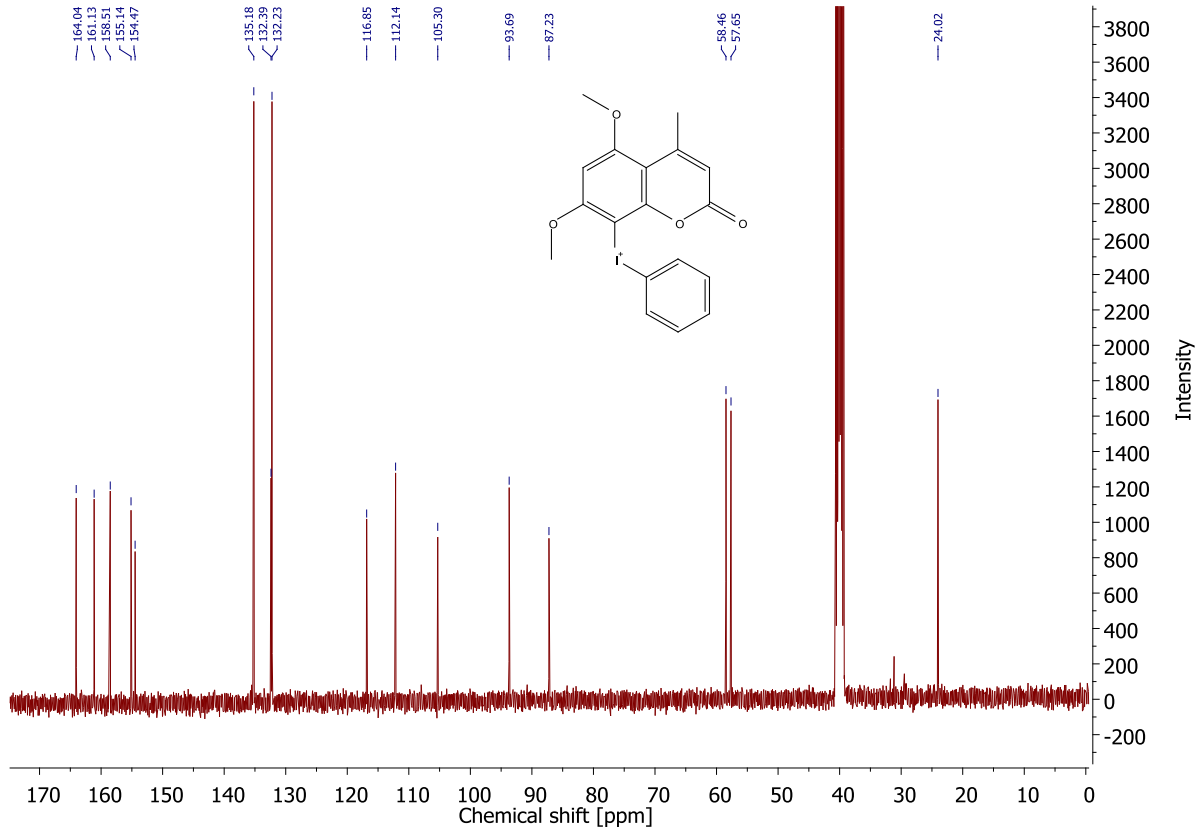

Figure S10: ^{13}C NMR of ***5,7M-P.***

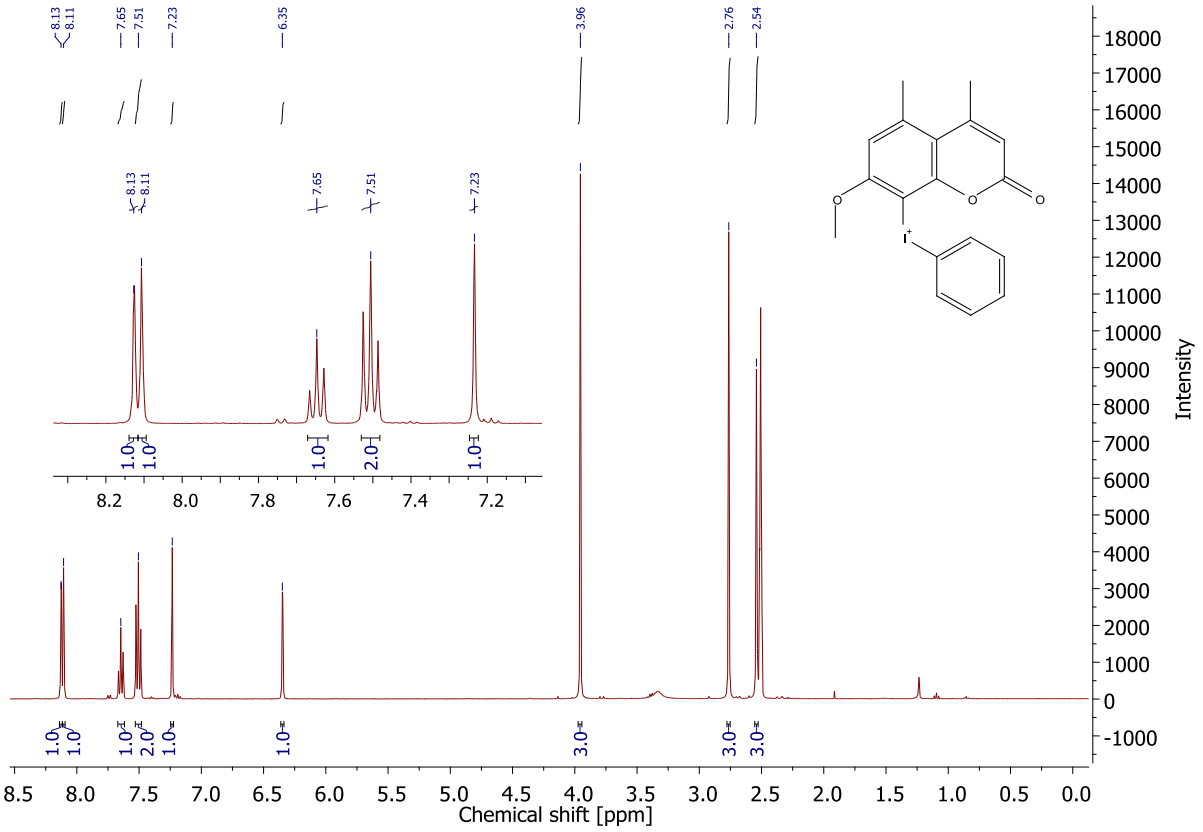

Figure S11: ^{1}H NMR of ***5Me-7M-P*** **.**

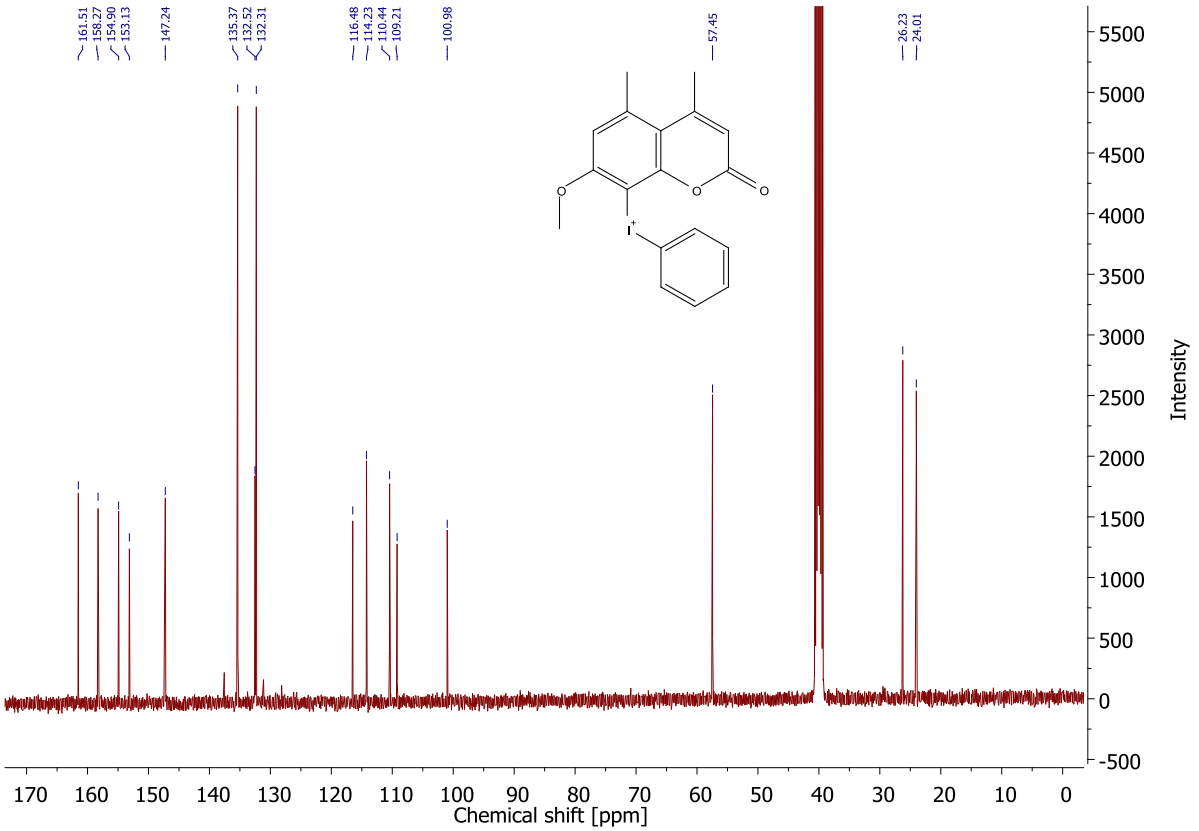

Figure S12: ^{13}C NMR of ***5Me-7M-P.***

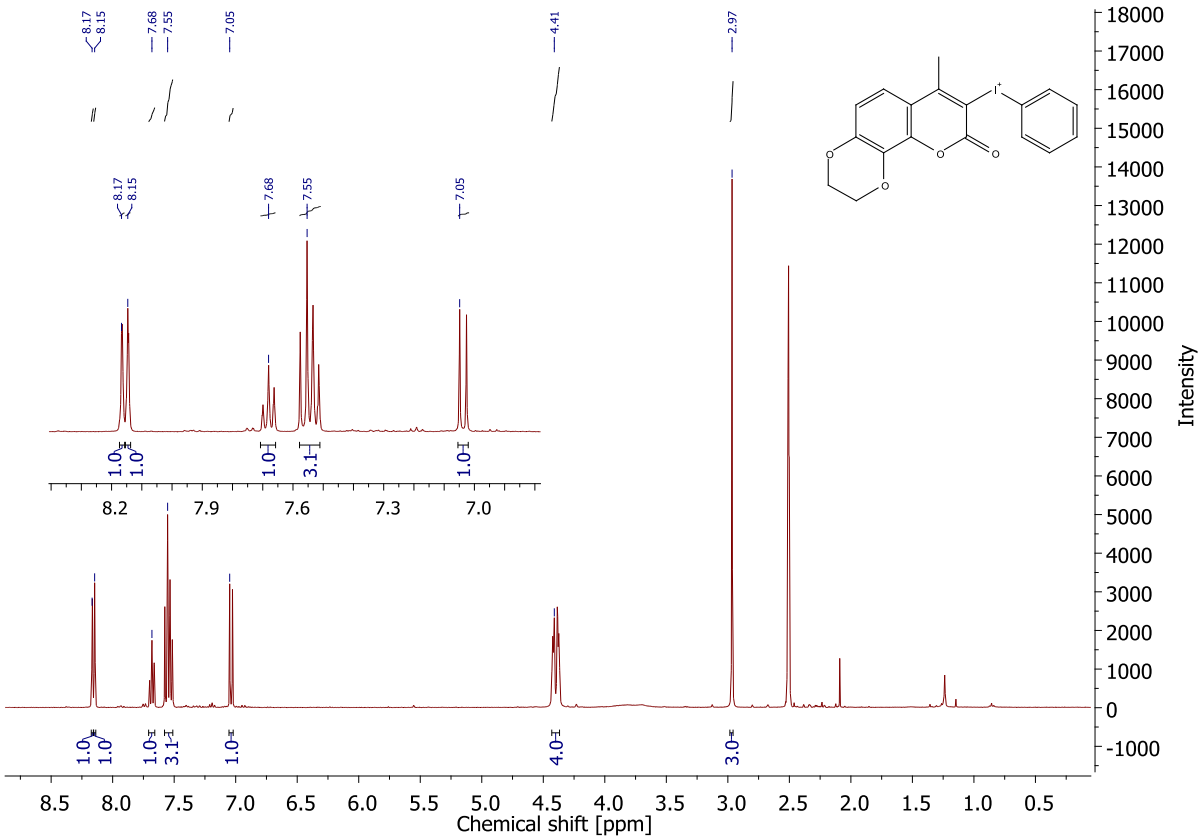

Figure S13: ^{1}H NMR of ***7,8ED-P.***

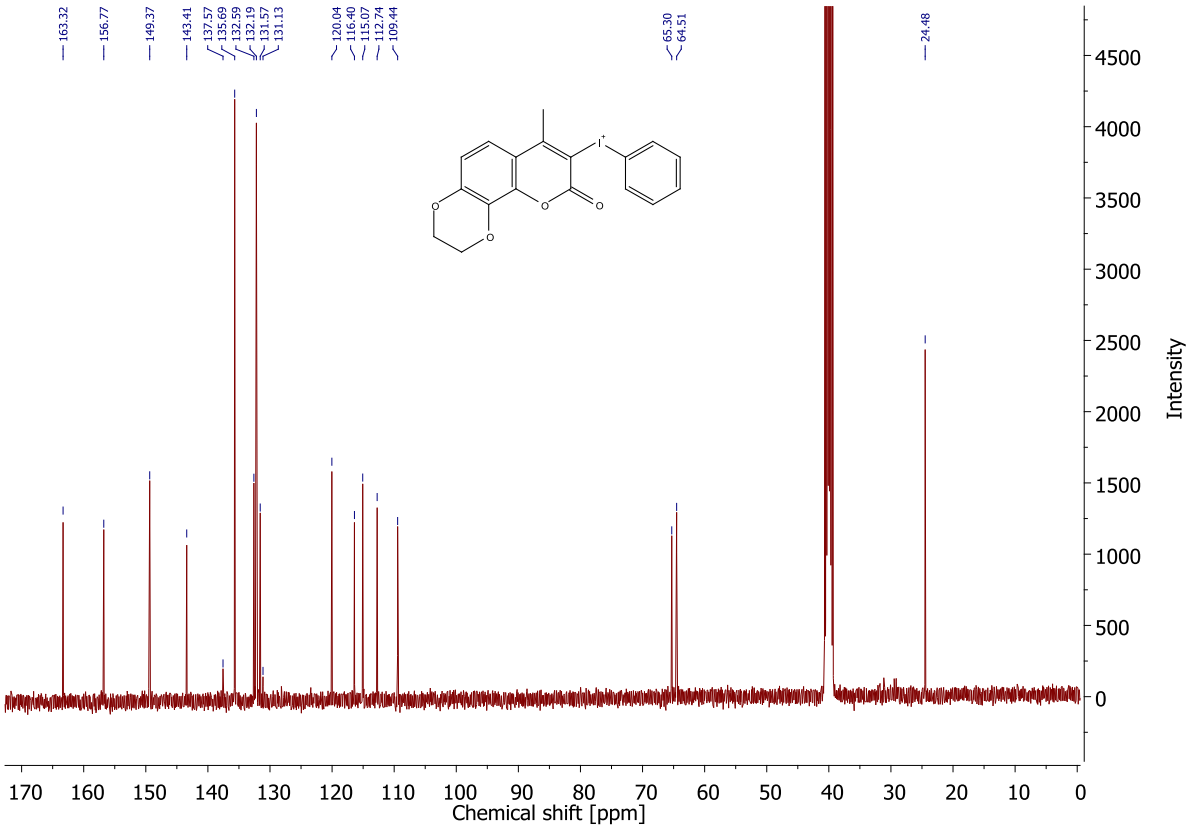

Figure S14: ^{13}C NMR of ***7,8ED-P.***

Section C. Additional photochemical and electrochemical data

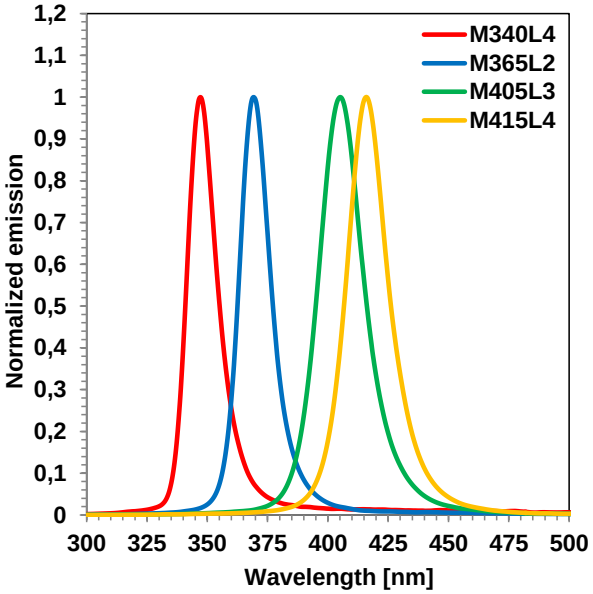

Figure S15: Normalized emission spectra of four LEDs used in measurements.

2. Comparison of absorption properties of iodonium salts with their chromophores.

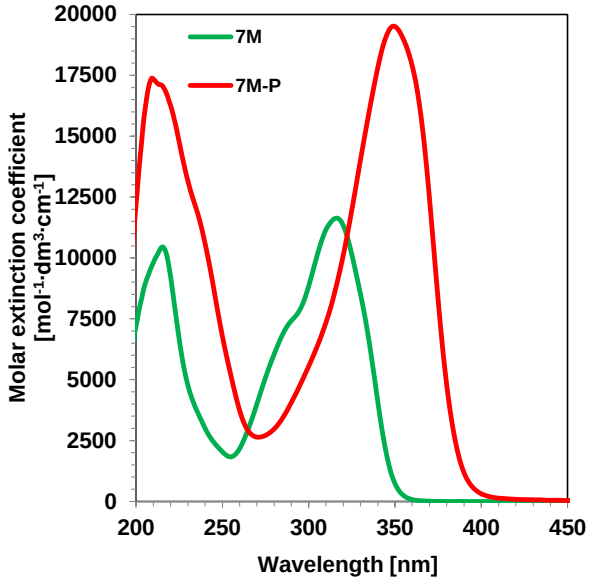

Figure S16. Comparison of UV-VIS absorption spectra of iodonium salt ***7M-P*** and its chromophore ***7M***.

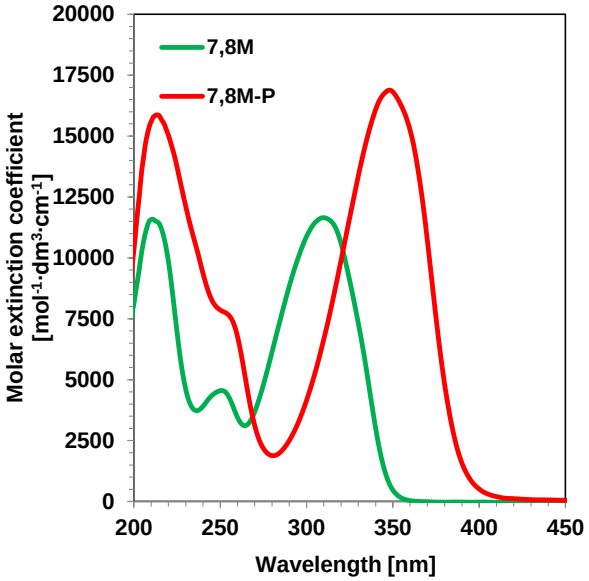

Figure S17. Comparison of UV-VIS absorption spectra of iodonium salt ***7,8M-P*** and its chromophore ***7,8M***.

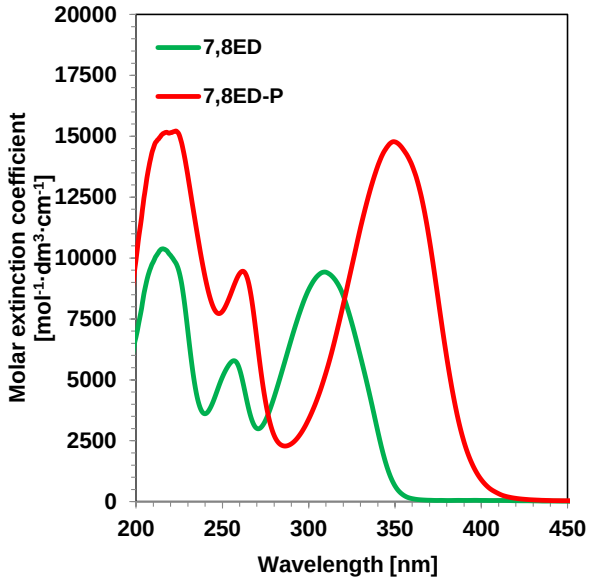

Figure S18. Comparison of UV-VIS absorption spectra of iodonium salt ***7,8ED-P*** and its chromophore ***7,8ED***.

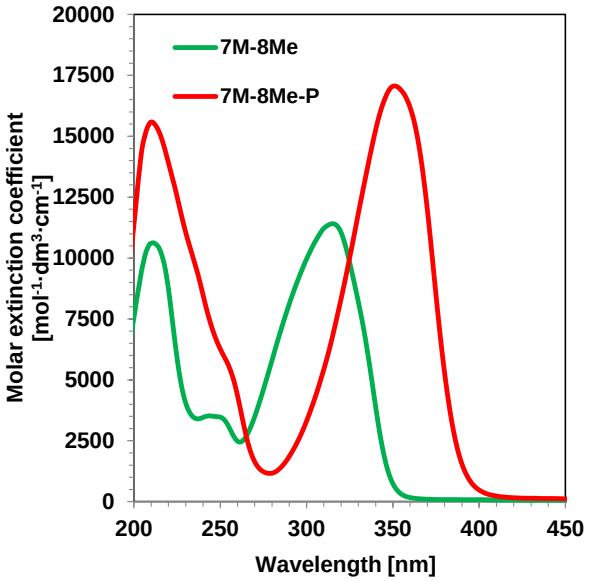

Figure S19. Comparison of UV-VIS absorption spectra of iodonium salt **7M-8Me-P** and its chromophore **7M-8Me**.

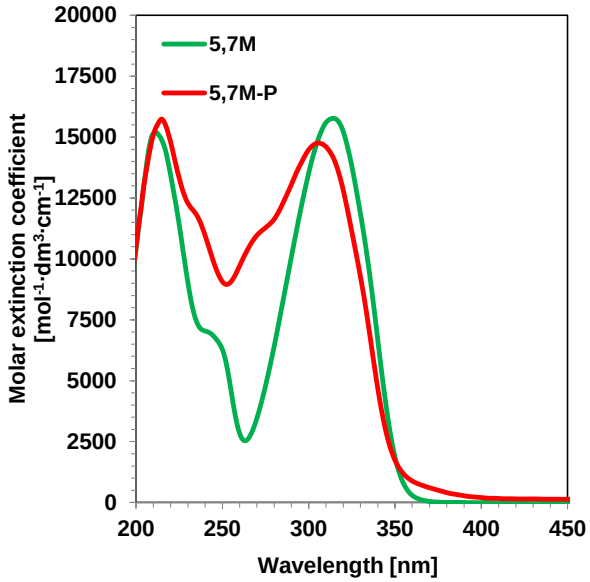

Figure S20. Comparison of UV-VIS absorption spectra of iodonium salt ***5,7M-P*** and its chromophore ***5,7M***.

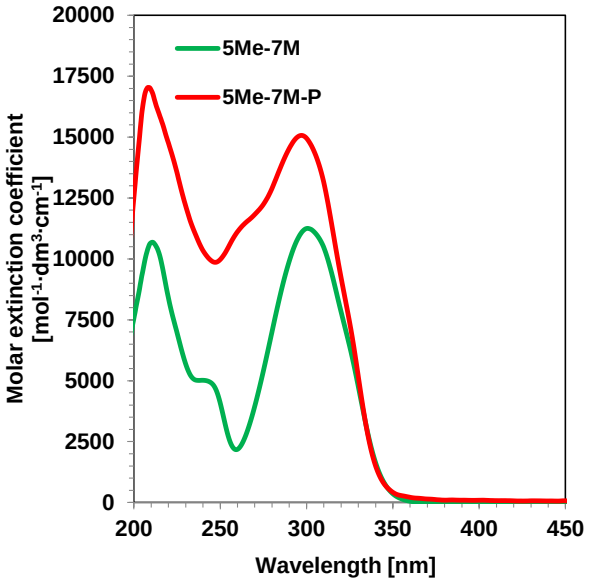

Figure S21. Comparison of UV-VIS absorption spectra of iodonium salt **5Me-7M-P** and its chromophore ***5Me-7M***.

Table S1. Comparison of spectral properties of chromophores and their iodonium salts in terms of absorption bands positions.

Compund	$\lambda_{max\text{-}ab}$ [nm]	$\Delta\lambda_{max}$ [nm]	Type of absorption shift
7M	316	33	Bathochromic shift
7M-P	349		
7,8M	314	34	Bathochromic shift
7,8M-P	348		
7,8ED	316	33	Bathochromic shift
7,8ED-P	349		
7M-8Me	315	35	Bathochromic shift
7M-8Me-P	350		
5,7M	314	9	Hypsochromic shift
5,7M-P	305		
5Me-7M	301	4	Hypsochromic shift
5Me-7M-P	297		

3. Steady state photolysis experiments

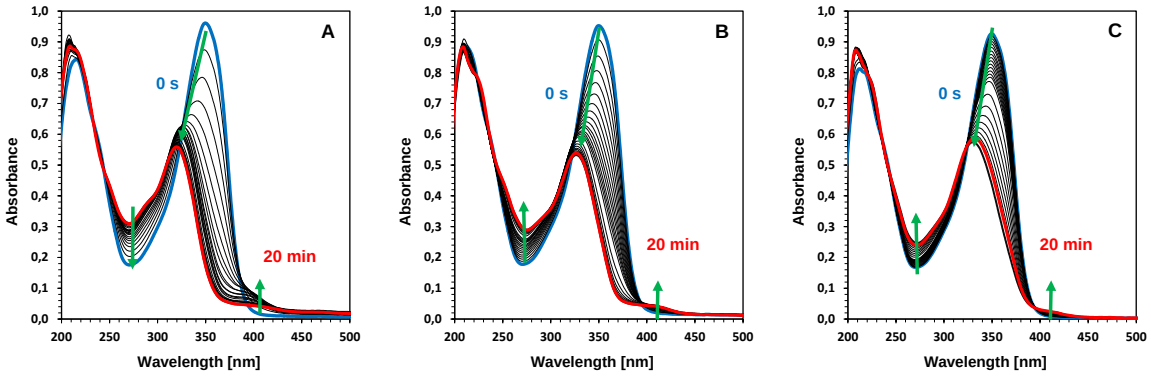

Figure S22. Photolysis of **7M-P** in acetonitrile upon exposure to LED at (A) 365 nm (3.6 mW/cm^2), (B) 405 nm (88.5 mW/cm^2), (C) 415 nm (117.0 mW/cm^2).

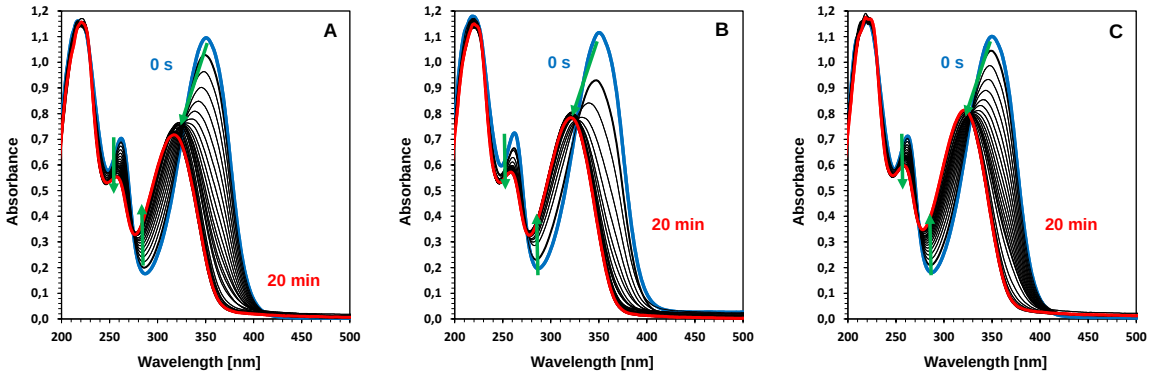

Figure S23. Photolysis of **7,8ED-P** in acetonitrile upon exposure to LED at (A) 365 nm (3.6 mW/cm^2), (B) 405 nm (88.5 mW/cm^2), (C) 415 nm (117.0 mW/cm^2).

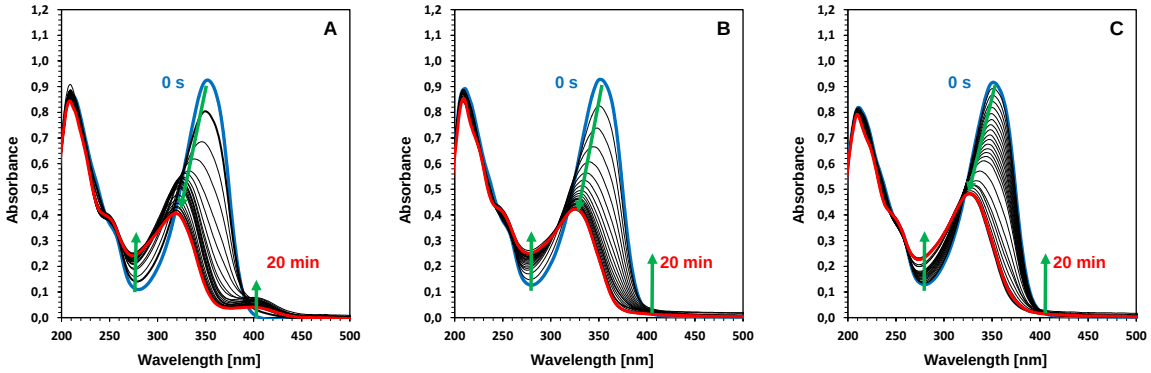

Figure S24. Photolysis of **7M-8Me-P** in acetonitrile upon exposure to LED at (A) 365 nm (3.6 mW/cm^2), (B) 405 nm (88.5 mW/cm^2), (C) 415 nm (117.0 mW/cm^2).

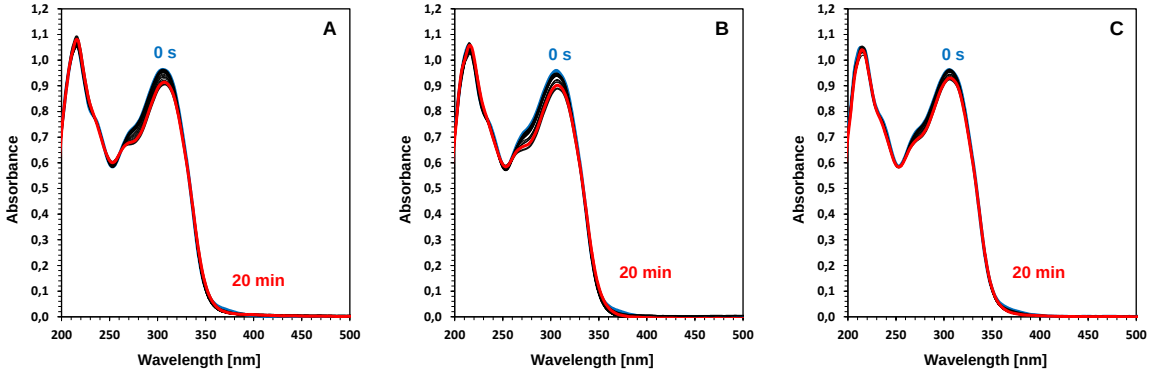

Figure S25. Photolysis of **5,7M-P** in acetonitrile upon exposure to LED at (A) 365 nm (3.6 mW/cm^2), (B) 405 nm (88.5 mW/cm^2), (C) 415 nm (117.0 mW/cm^2).

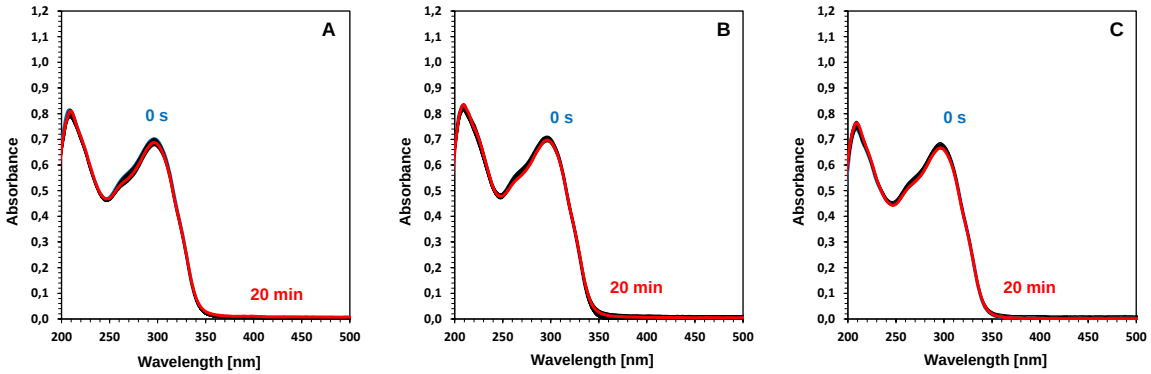

Figure S26. Photolysis of **5Me-7M-P** in acetonitrile upon exposure to LED at (A) 365 nm (3.6 mW/cm^2), (B) 405 nm (88.5 mW/cm^2), (C) 415 nm (117.0 mW/cm^2).

4. Reduction potential measurements of new coumarin iodonium salts

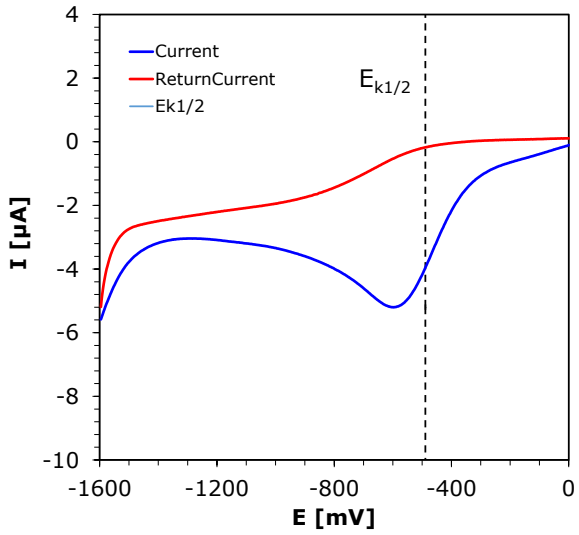

Figure S27. Cyclic voltammogram curves of the **7M-P** reduction in acetonitrile.

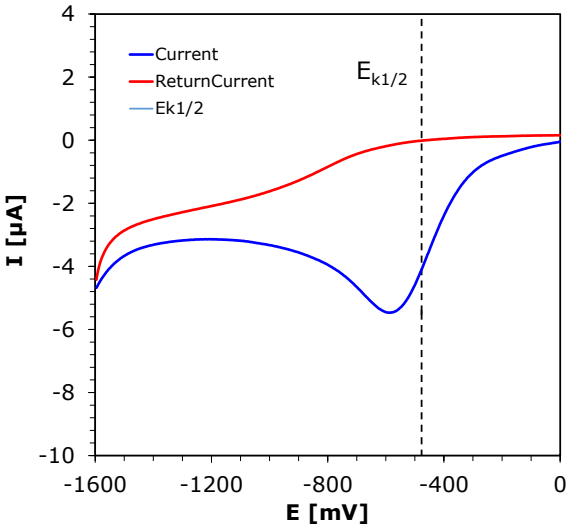

Figure S28. Cyclic voltammogram curves of the **7,8ED-P** reduction in acetonitrile

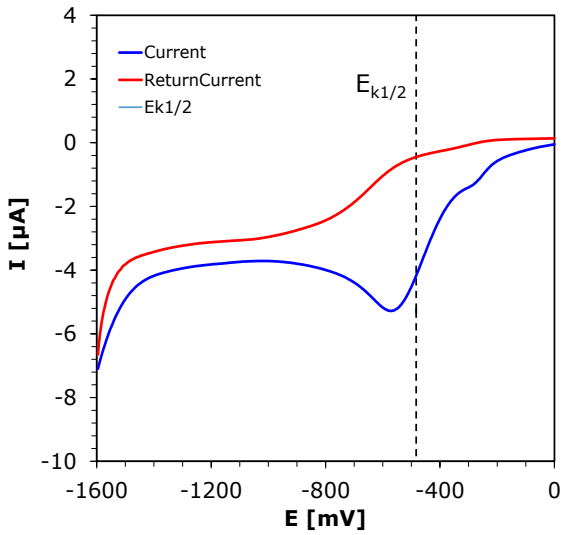

Figure S29. Cyclic voltammogram curves of the **7,8M-P** reduction in acetonitrile.

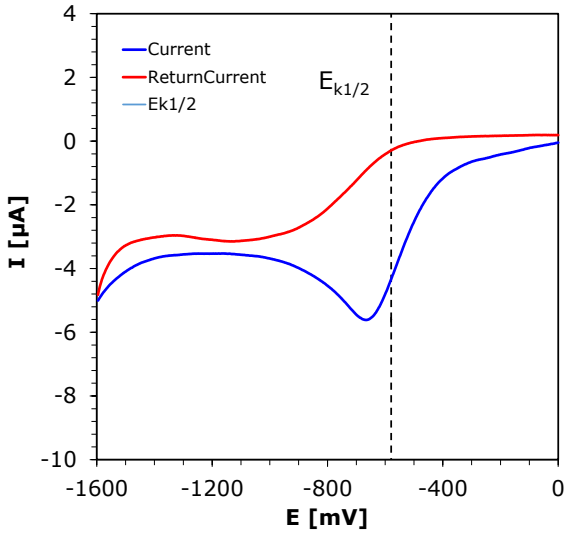

Figure S30. Cyclic voltammogram curves of the **5Me-7M-P** reduction in acetonitrile

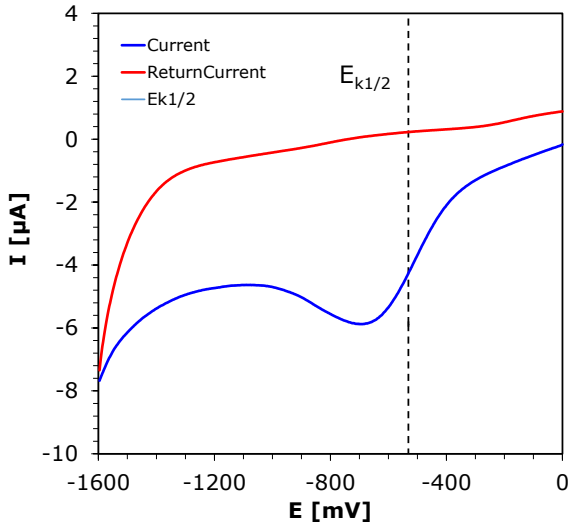

Figure S31. Cyclic voltammogram curves of the **7M-8Me-P** reduction in acetonitrile.

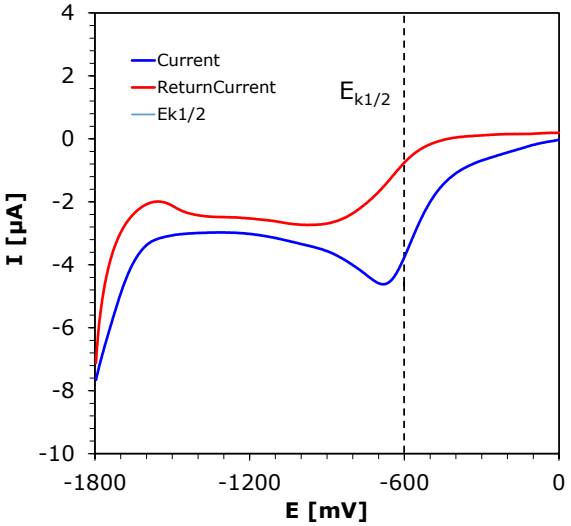

Figure S32. Cyclic voltammogram curves of the **5,7M-P** reduction in acetonitrile.

5. Quantum efficiency of acid generation

Quantum yield was determined making one assumption:

$$n_{abs} = n_{emit}$$

,where:
- n_{abs} – amount of photons absorbed by irradiated sample
- n_{emit} – amount of photons emitted by used light source

Measured iodonium salts were dissolved in acetonitrile in concentration ensuring absorbance of solution greater than 2.5 in whole emission range of used LED@340nm. This absorbance ensures a nearly 100% absorption of the incident photons. Thus, the amount of absorbed photons is known and allows to determine quantum efficiency using following equation:

$$\phi_{HA} = \frac{[HA]}{n_{abs}} = \frac{[HA]}{n_{emit}}$$

,where:
- [HA] – concentration of acid generated during irradation of sample
- n_{abs} – amount of photons absorbed by irradiated sample
- n_{emit} – amount of photons emitted by used light source

Amount of generated acid was determined using rhodamine B base as acid indicator. Based on rhodamine B ability to significantly change the absorption spectra (Figure S33) the calibration curve was prepared using *p*-toluenosulfonic acid as an acid standard. Measurements were carried out in acetonitrile and absorbance at 555nm was monitored (Figure S34).

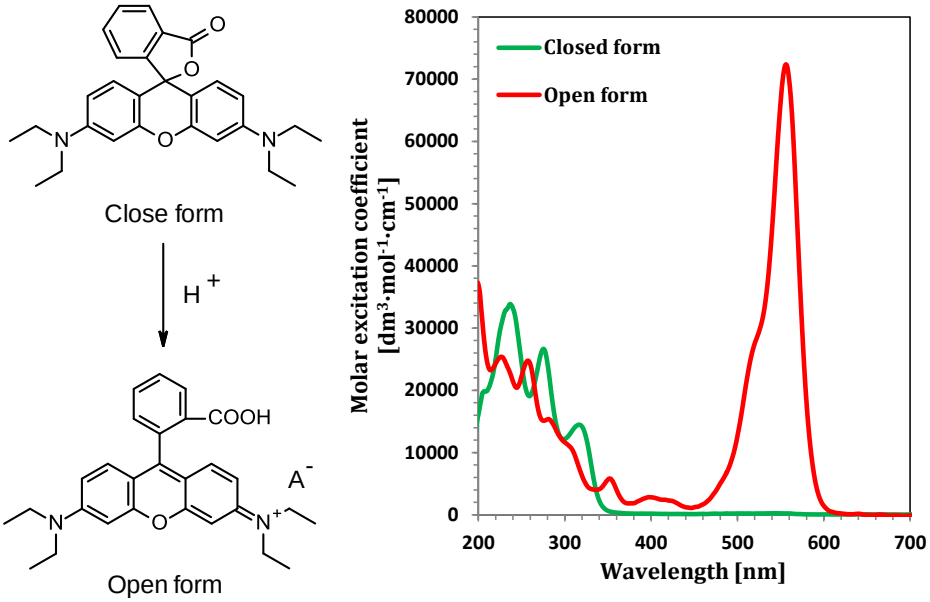

Figure S33. Opening of Rhodamine B base (left) and absorption spectrum of both forms of this compound (right).

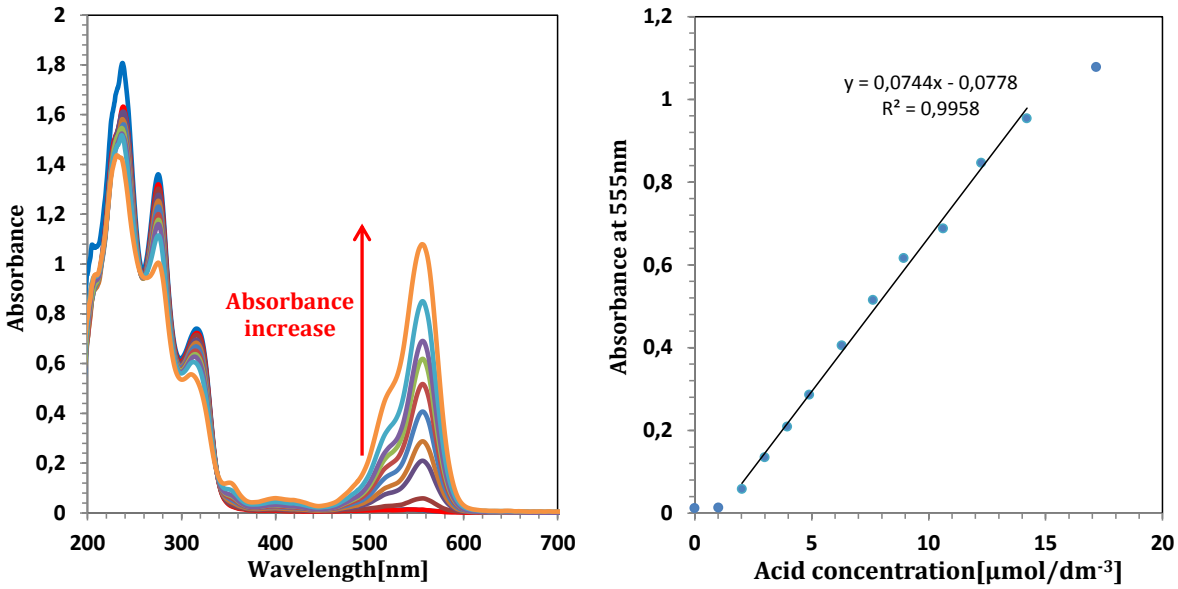

Figure S34. Behavior of absorbance spectra of Rhodamine B base during acid titration (left) and prepared calibration curve (right).

6. Performance of the coumarin derivatives as photoinitiators for cationic photopolymerization

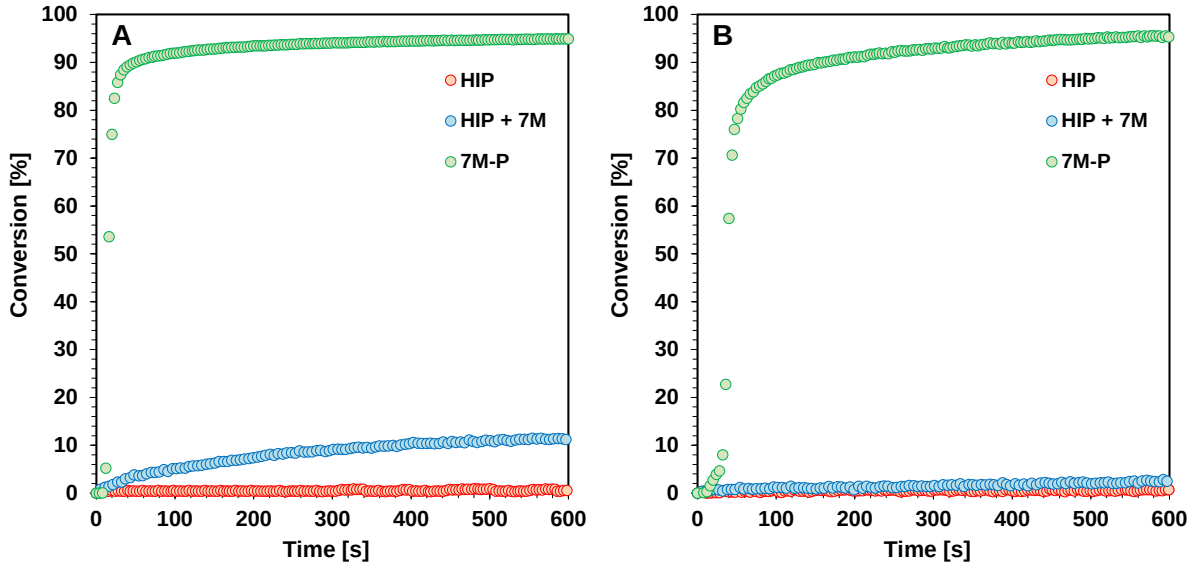

Figure S35. The comparison of photopolymerization profiles of HIP, HIP + 7M and 7M-P (1% wt. each) in TEGDVE under irradiation of LED@365nm (A) and LED@405nm (B). The activity of HIP and HIP + 7M compared to 7M-P is negligible.

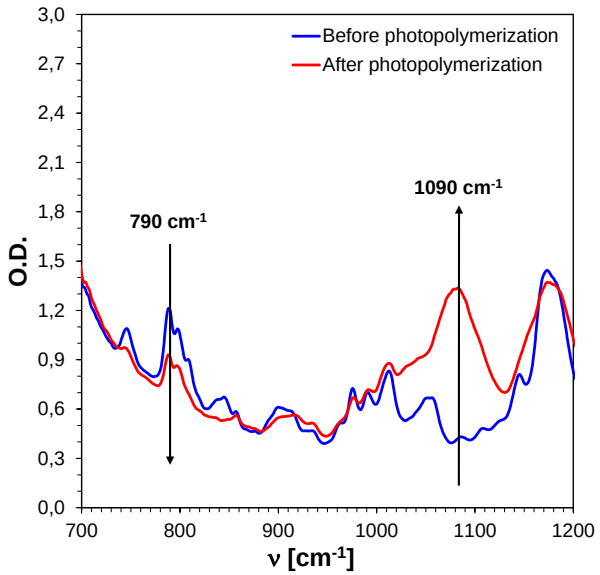

Figure S36. Spectra before and after photopolymerization of epoxy monomer CADE with initiator **7M-P** under LED@365nm irradiation.

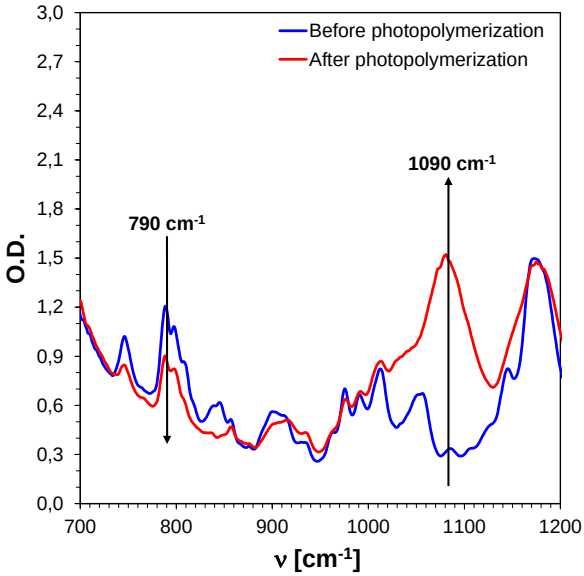

Figure S37. Spectra before and after photopolymerization of epoxy monomer CADE with initiator **7,8M-P** under LED@365nm irradiation.

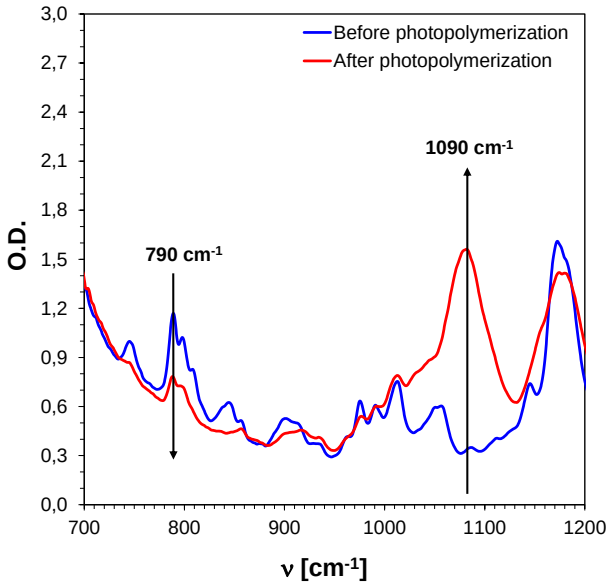

Figure S38. Spectra before and after photopolymerization of epoxy monomer CADE with initiator **7,8ED-P** under LED@365nm irradiation.

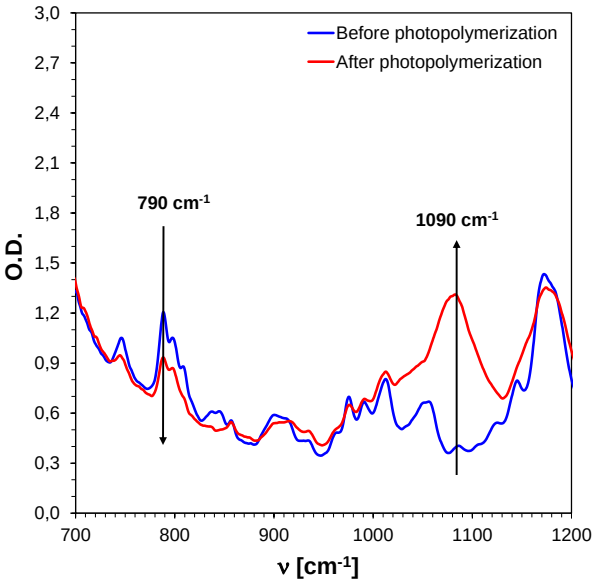

Figure S39. Spectra before and after photopolymerization of epoxy monomer CADE with initiator **7M-8Me-P** under LED@365nm irradiation.

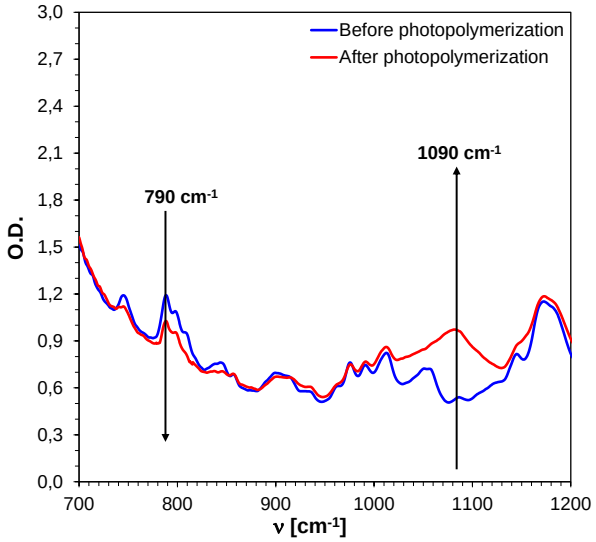

Figure S40. Spectra before and after photopolymerization of CADE with initiator **5,7M-P** under LED@365nm.

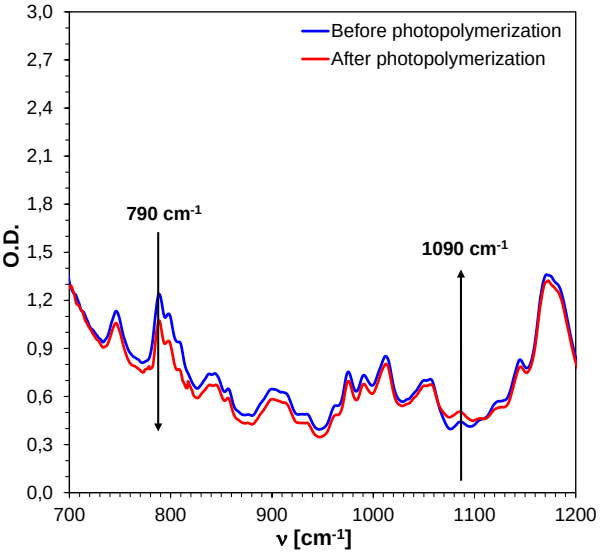

Figure S41. Spectra before and after photopolymerization of CADE with initiator **5Me-7M-P** under LED@365nm.

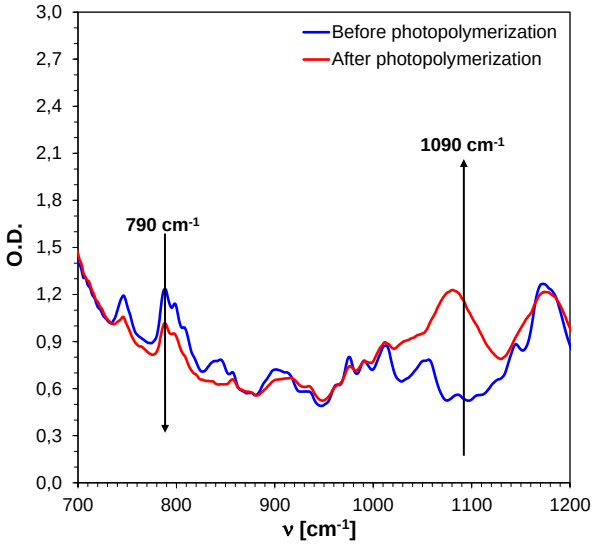

Figure S42. Spectra before and after photopolymerization of epoxy monomer CADE with initiator **7M-P** under LED@405nm irradiation.

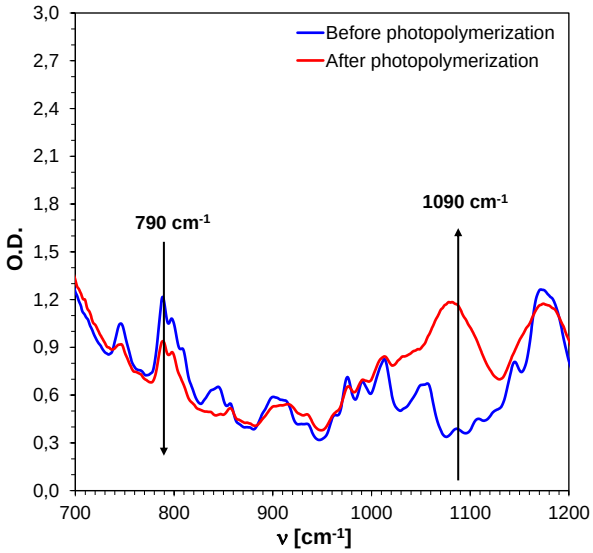

Figure S43. Spectra before and after photopolymerization of epoxy monomer CADE with initiator **7,8M-P** under LED@405nm irradiation.

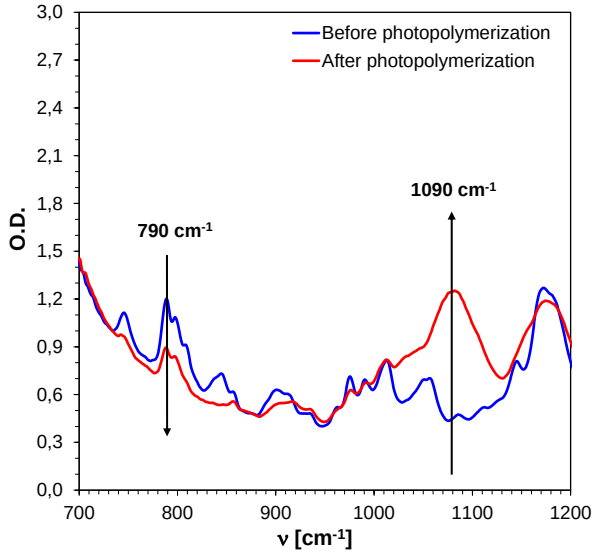

Figure S44. Spectra before and after photopolymerization of CADE with initiator **7,8ED-P** under LED@405nm.

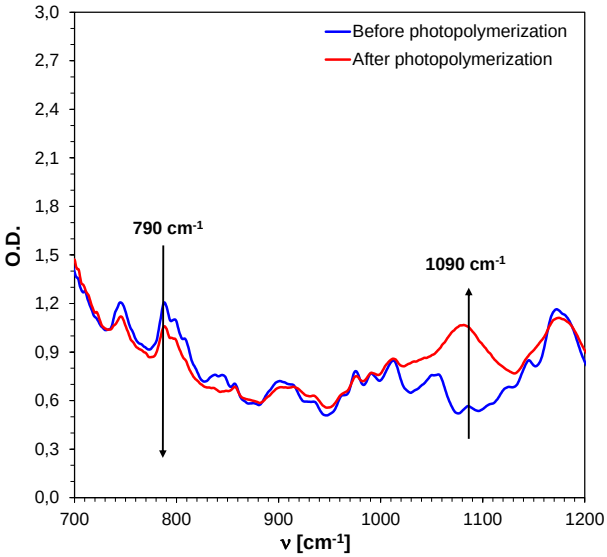

Figure S45. Spectra before and after photopolymerization of CADE with initiator **7M-8Me-P** under LED@405nm.

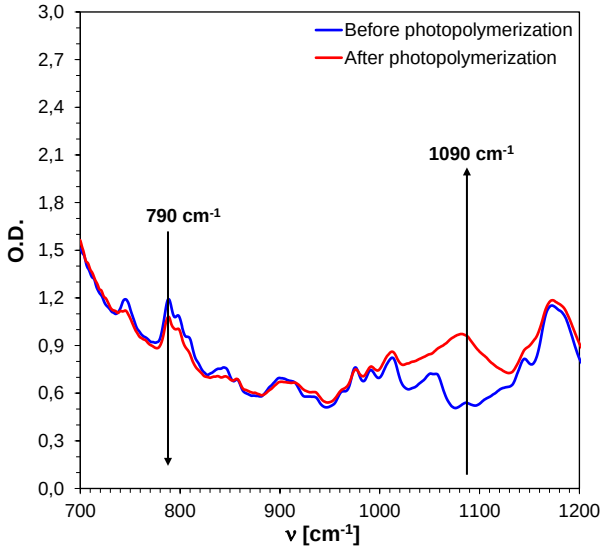

Figure S46. Spectra before and after photopolymerization of CADE with initiator **5,7M-P** under LED@405nm irradiation.

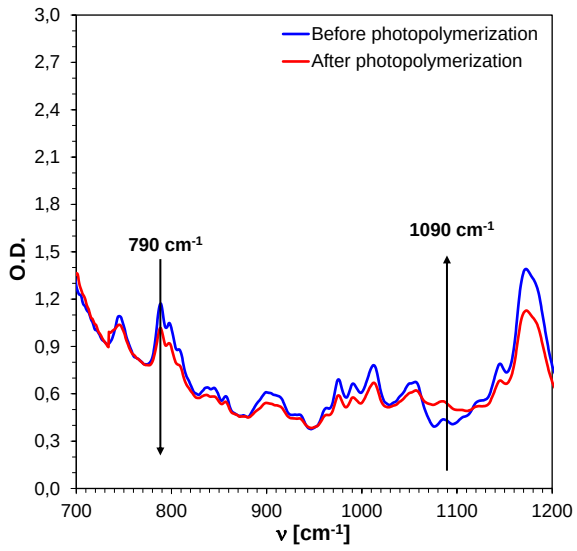

Figure S47. Spectra before and after photopolymerization of CADE with initiator **5Me-7M-P** under LED@405nm.

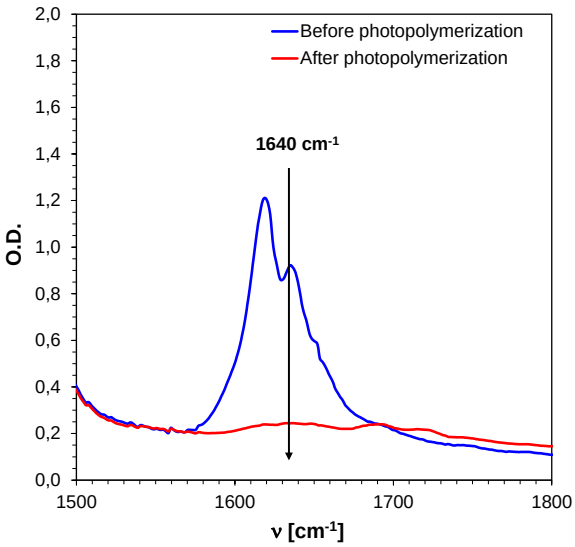

Figure S48. Spectra before and after photopolymerization of vinyl monomer TEGDVE with initiator **7M-P** under LED@365nm irradiation.

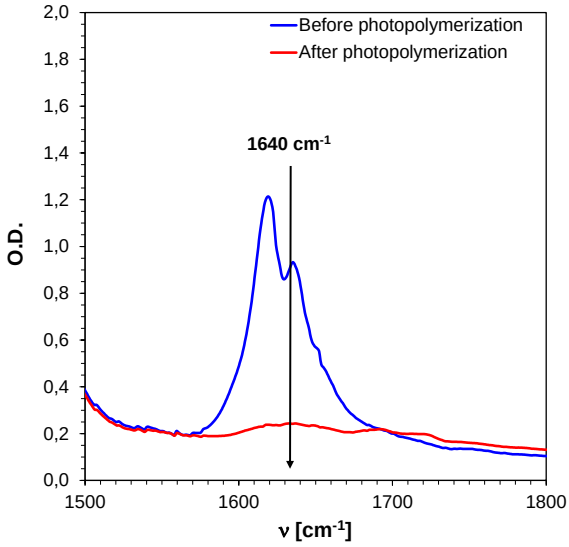

Figure S49. Spectra before and after photopolymerization of vinyl monomer TEGDVE with initiator **7,8M-P** under LED@365nm irradiation.

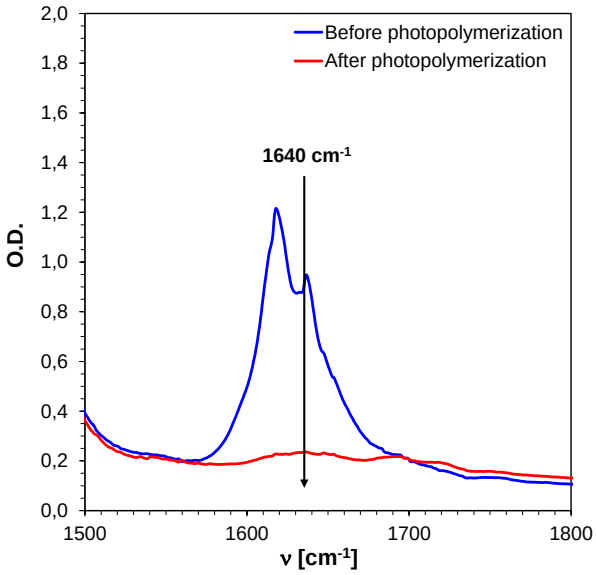

Figure S50. Spectra before and after photopolymerization of vinyl monomer TEGDVE with initiator **7,8ED-P** under LED@365nm irradiation.

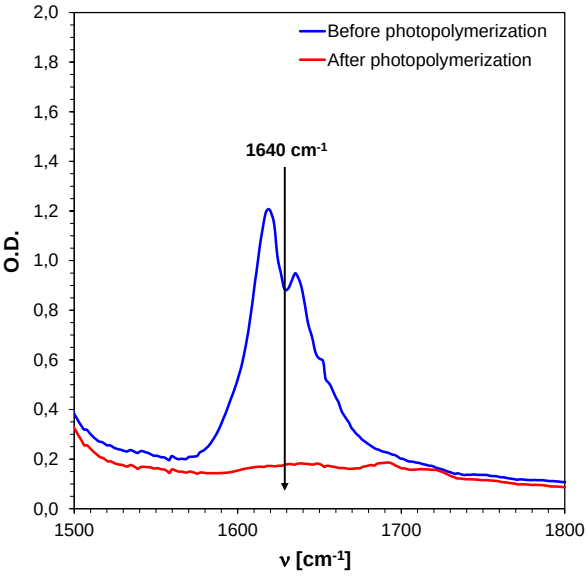

Figure S51. Spectra before and after photopolymerization of vinyl monomer TEGDVE with initiator **7M-8Me-P** under LED@365nm irradiation.

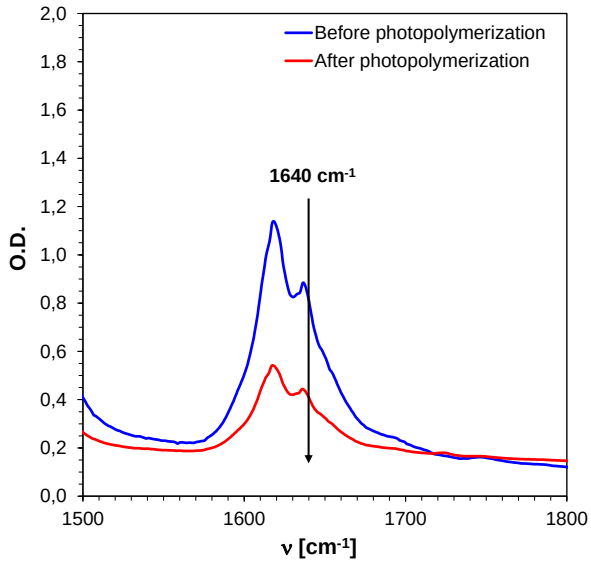

Figure S52. Spectra before and after photopolymerization of TEGDVE with initiator **5,7M-P** under LED@365nm.

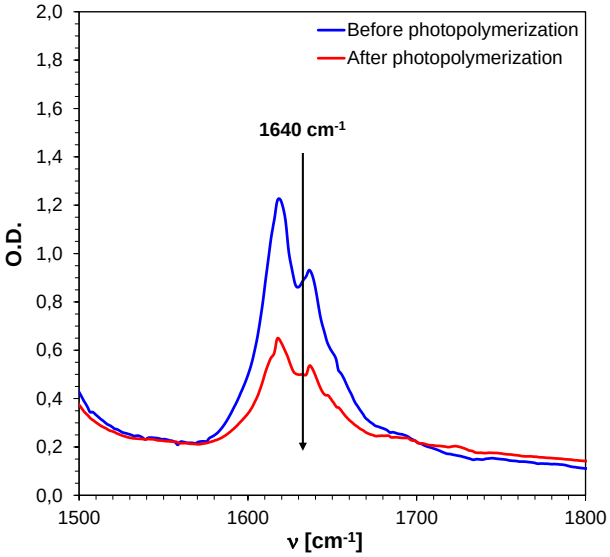

Figure S53. Spectra before and after photopolymerization of TEGDVE with initiator **5Me-7M-P** under LED@365nm.

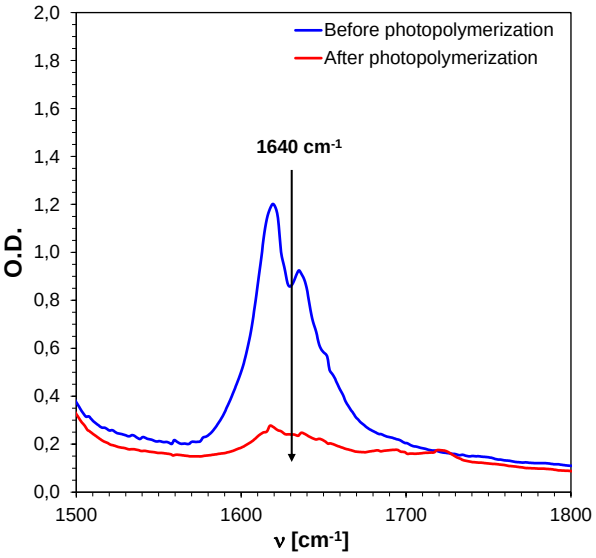

Figure S54. Spectra before and after photopolymerization of TEGDVE with initiator **7M-P** under LED@405nm.

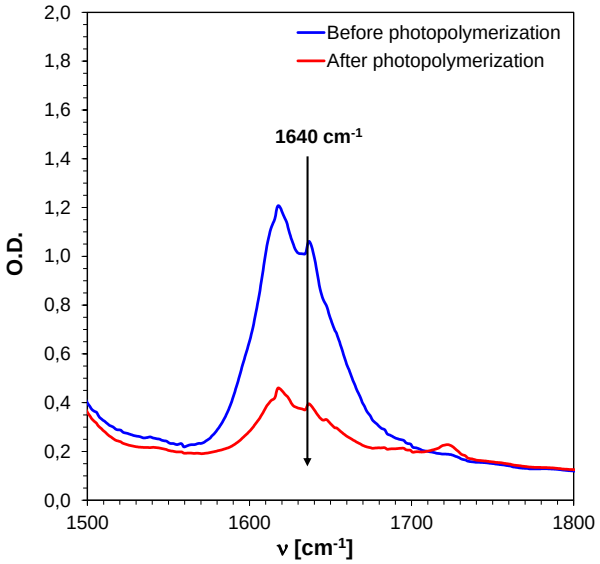

Figure S55. Spectra before and after photopolymerization of TEGDVE with initiator **7,8M-P** under LED@405nm.

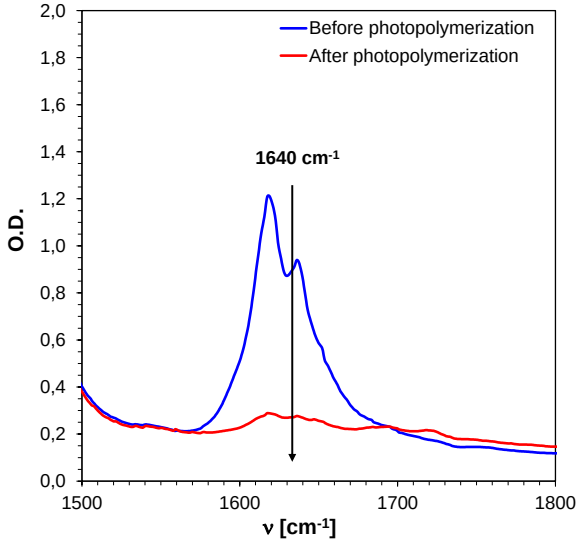

Figure S56. Spectra before and after photopolymerization of TEGDVE with initiator **7,8ED-P** under LED@405nm.

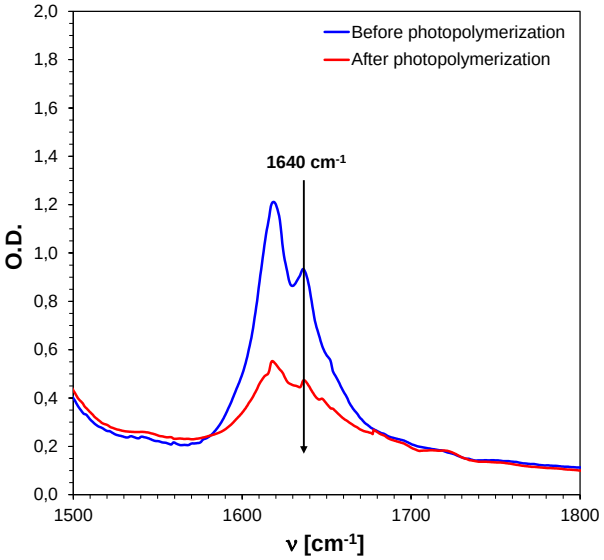

Figure S57. Spectra before and after photopolymerization of TEGDVE with initiator **7M-8Me-P** under LED@405nm.

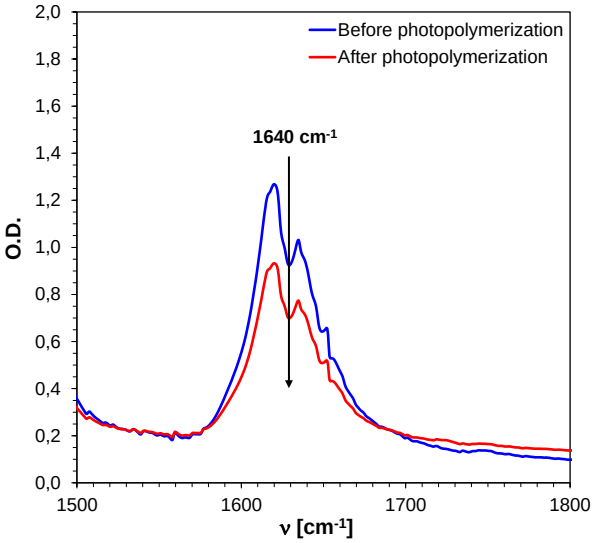

Figure S58. Spectra before and after photopolymerization of vinyl monomer TEGDVE with initiator **5,7M-P** under LED@405nm irradiation.

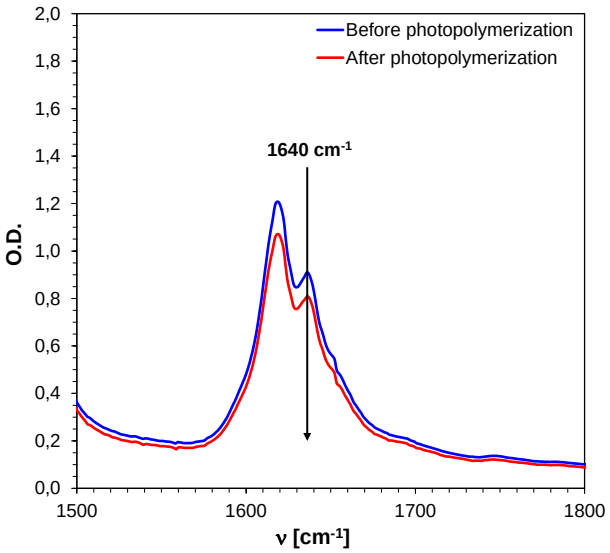

Figure S59. Spectra before and after photopolymerization of vinyl monomer TEGDVE with initiator **5Me-7M-P** under LED@405nm irradiation.

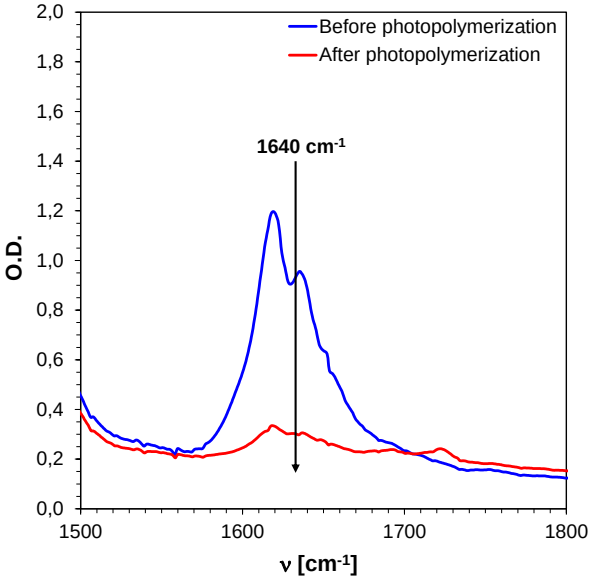

Figure S60. Spectra before and after photopolymerization of TEGDVE with initiator **7M-P** under LED@415nm.

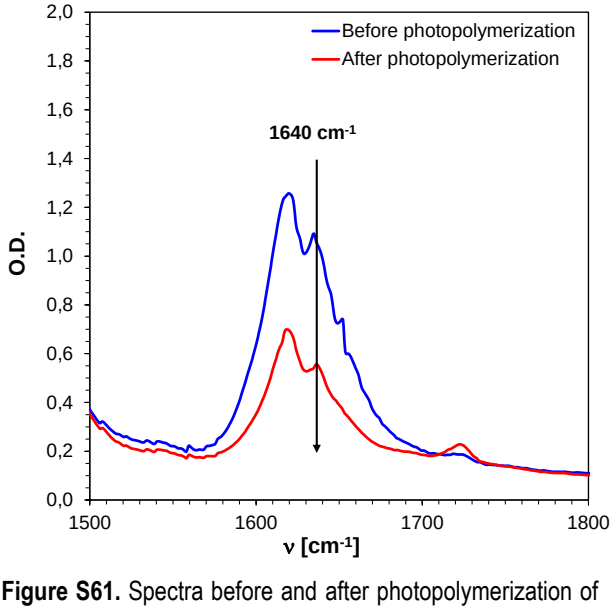

Figure S61. Spectra before and after photopolymerization of TEGDVE with initiator **7,8M-P** under LED@415nm.

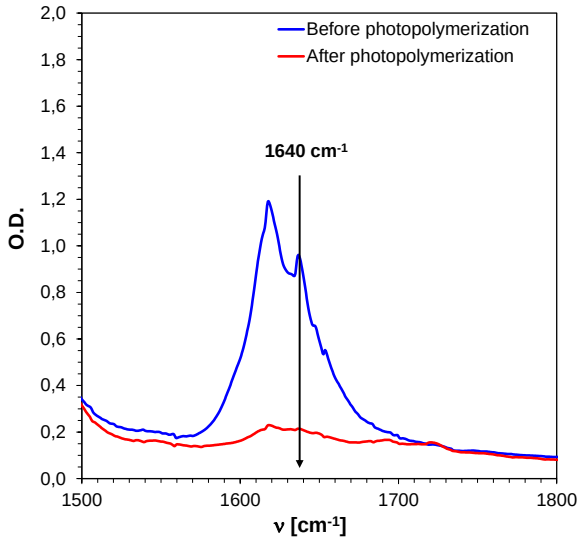

Figure S62. Spectra before and after photopolymerization of TEGDVE with initiator **7,8ED-P** under LED@415nm.

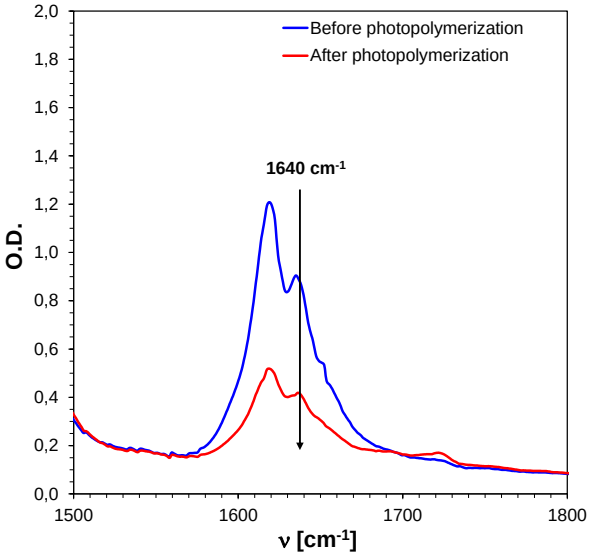

Figure S63. Spectra before and after photopolymerization of TEGDVE with initiator **7M-8Me-P** under LED@415nm.

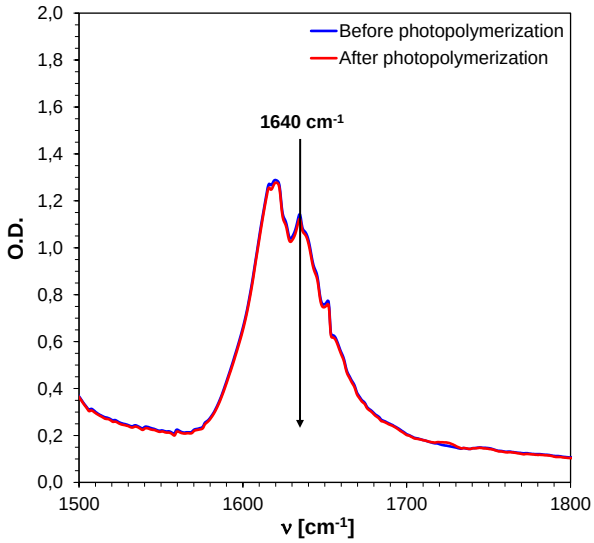

Figure S64. Spectra before and after photopolymerization of TEGDVE with initiator **5,7M-P** under LED@415nm.

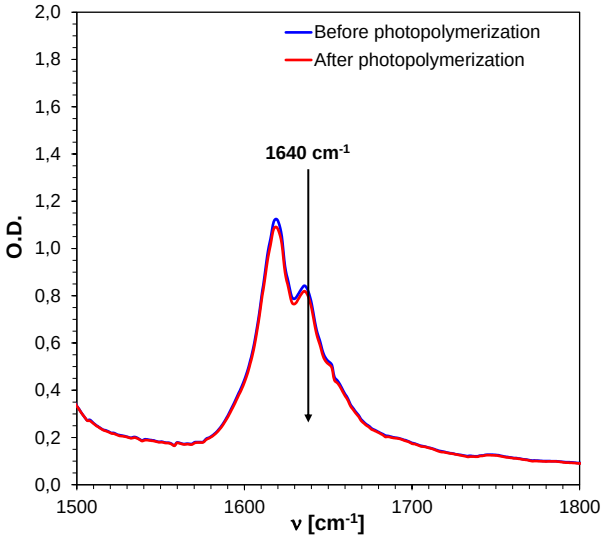

Figure S65. Spectra before and after photopolymerization of TEGDVE with initiator **5Me-7M-P** under LED@415nm.

7. Photo Differential Scanning Calorimetry measurements of coumarin based iodonium salt activity.

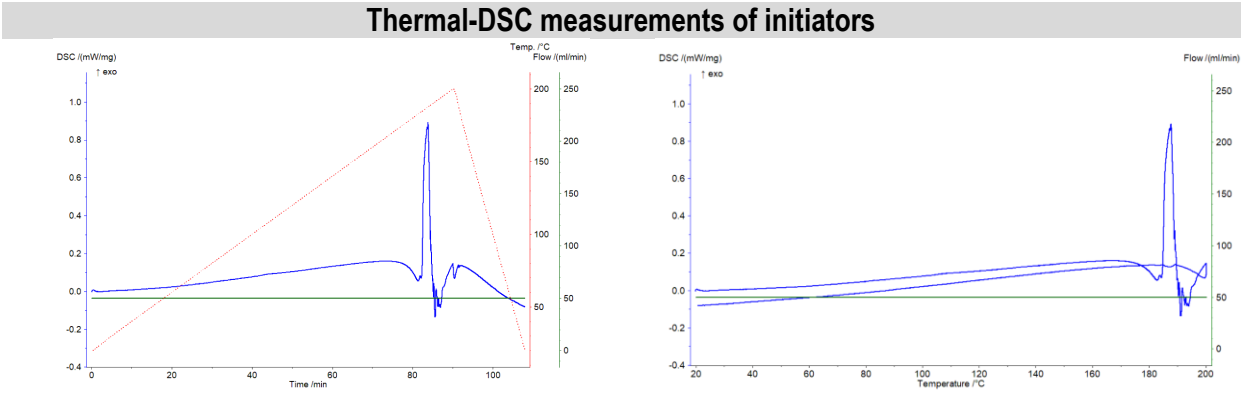

Figure S66. DSC signal obtained during thermal measurements of **7M-P** initiator (a) time-dependent, (b) temerature-dependent.

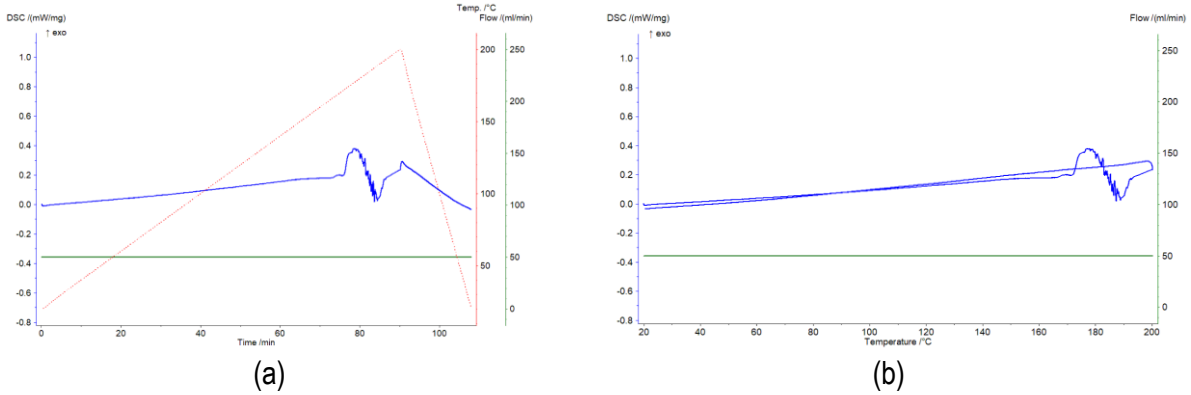

Figure S67. DSC signal obtained during thermal measurements of **7,8M-P** initiator (a) time-dependent, (b) temerature-dependent.

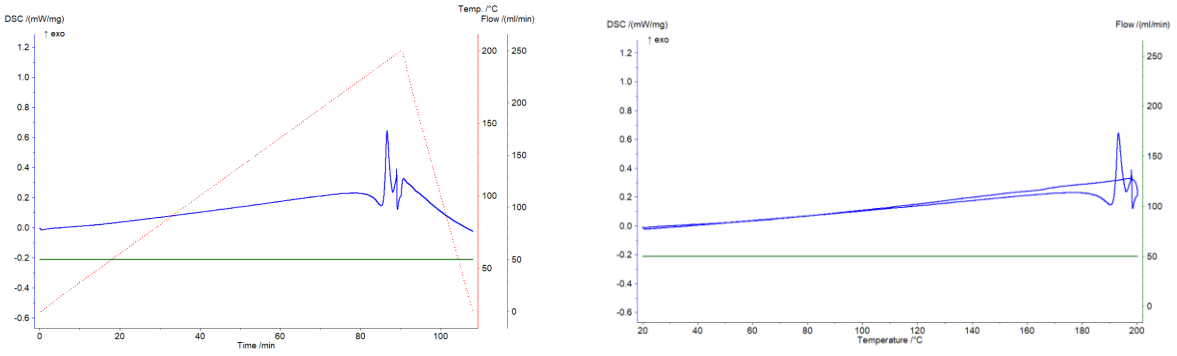

(a) (b)

Figure S68. DSC signal obtained during thermal measurements of **7,8ED-P** initiator (a) time-dependent, (b) temerature-dependent.

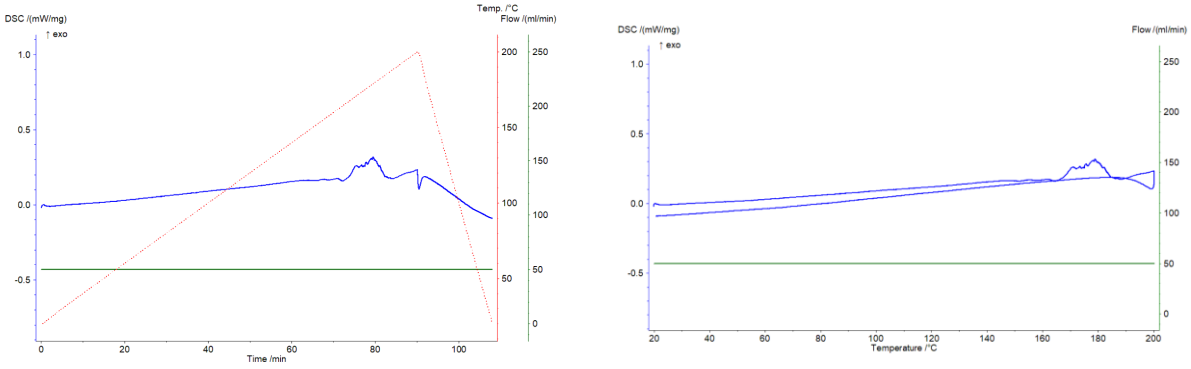

(a) (b)

Figure S69. DSC signal obtained during thermal measurements of **7M-8Me-P** initiator (a) time-dependent, (b) temerature-dependent.

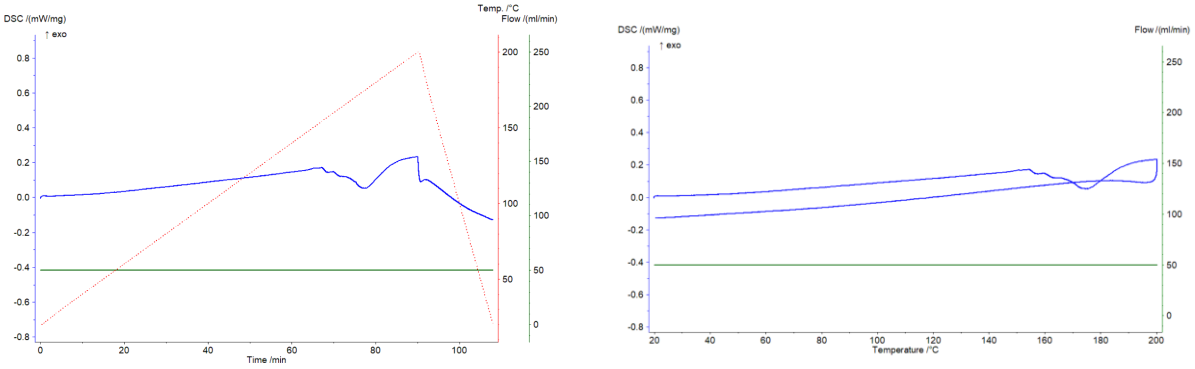

(a) (b)

Figure S70. DSC signal obtained during thermal measurements of **5,7M-P** initiator (a) time-dependent, (b) temerature-dependent.

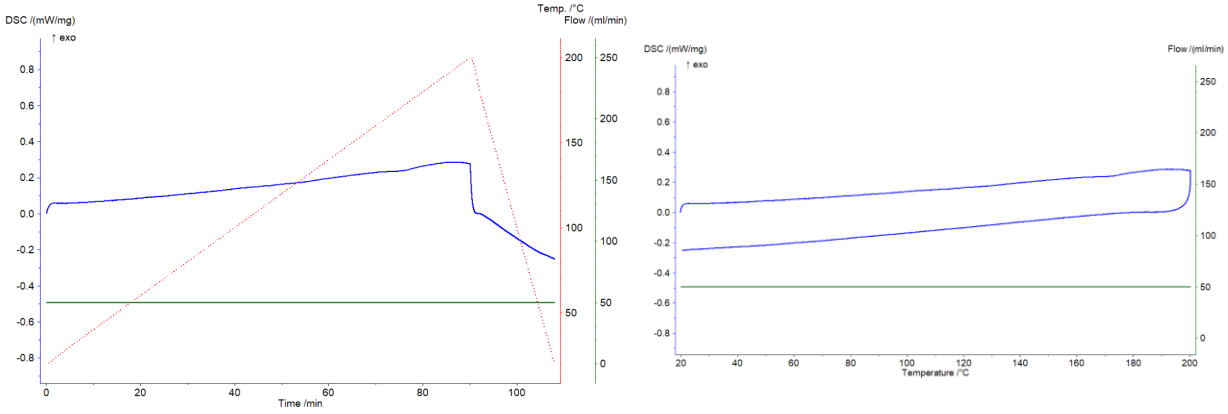

(a) (b)

Figure S71. DSC signal obtained during thermal measurements of **5Me-7M-P** initiator (a) time-dependent, (b) temerature-dependent.

Thermal measurements of resins (initiator + TEGDVE)

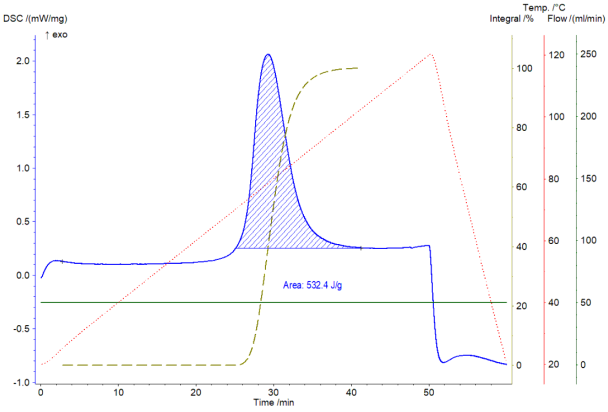

Figure S72. DSC signal obtained during thermal measurements of resin: **7M-P** and TEGDVE

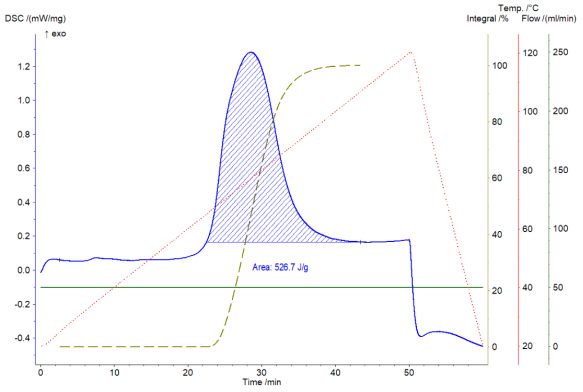

Figure S73. DSC signal obtained during thermal measurements of resin: **7,8M-P** and TEGDVE

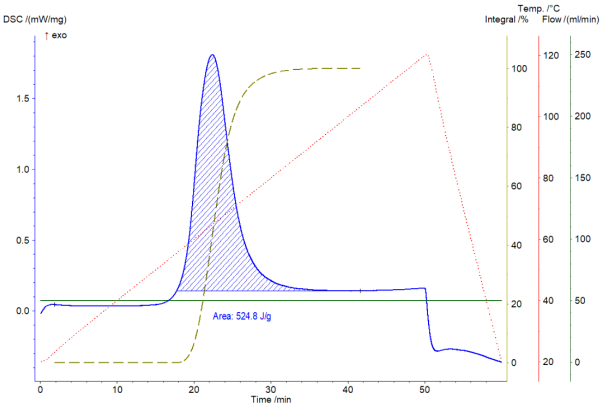

Figure S74. DSC signal obtained during thermal measurements of resin: **7,8ED-P** and TEGDVE

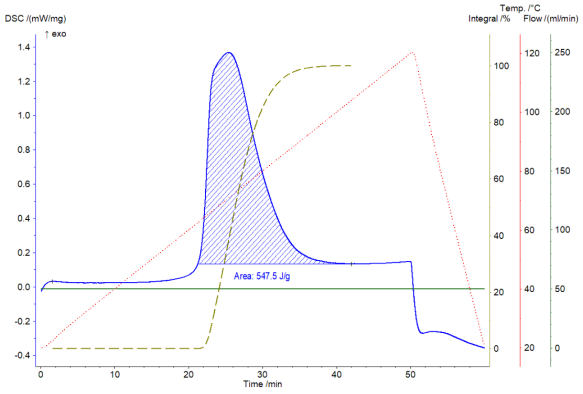

Figure S75. DSC signal obtained during thermal measurements of resin: **7M-8Me-P** and TEGDVE

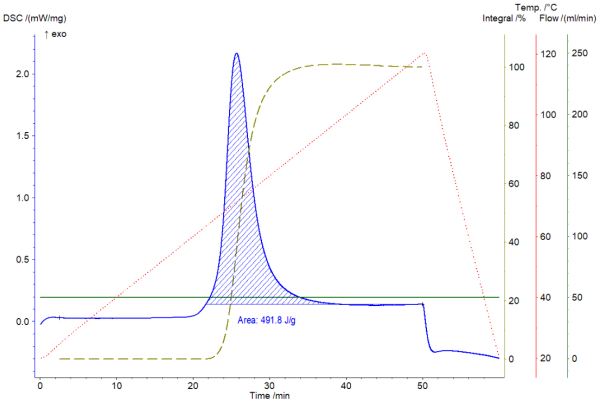

Figure S76. DSC signal obtained during thermal measurements of resin: **5,7M-P** and TEGDVE

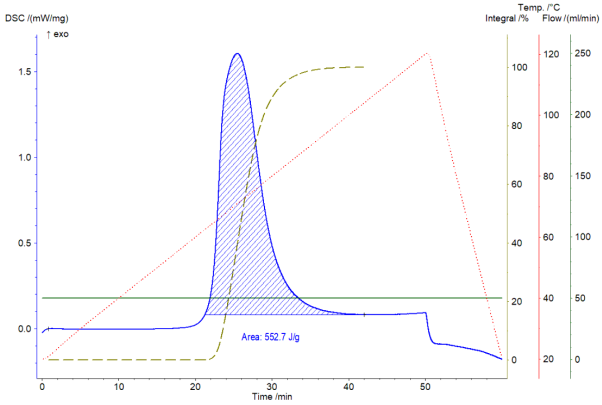

Figure S77. DSC signal obtained during thermal measurements of resin: **5Me-7M-P** and TEGDVE

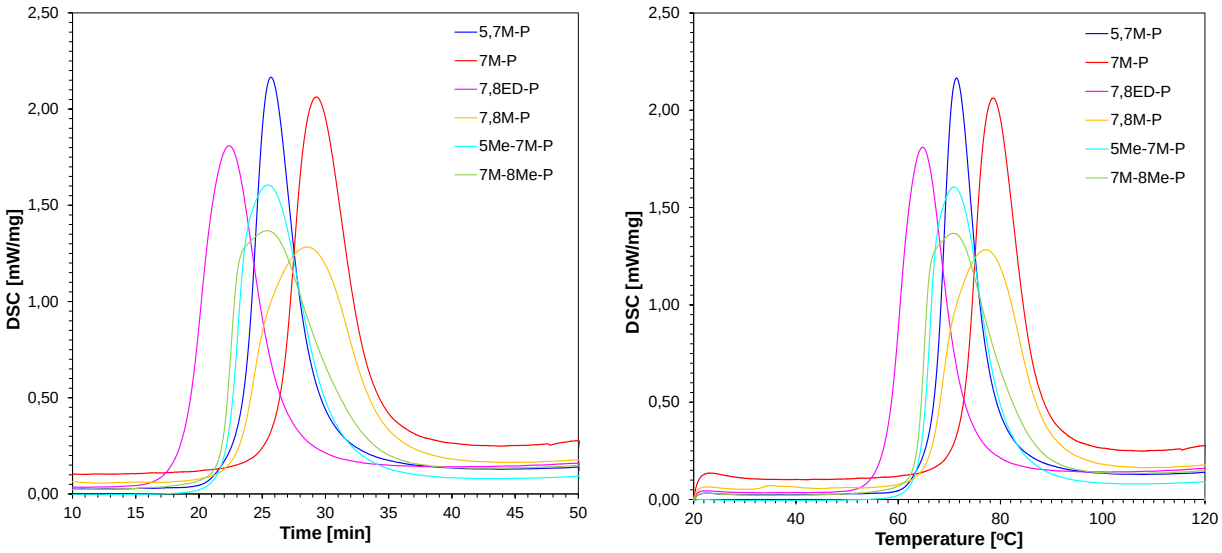

(a) (b)

Figure S78. Thermal DSC measurements of cationic resins (initiator + TEGDVE): (a) time-dependent, (b) temerature-dependent.

Photo-DSC measurements of cationic oxetane resins

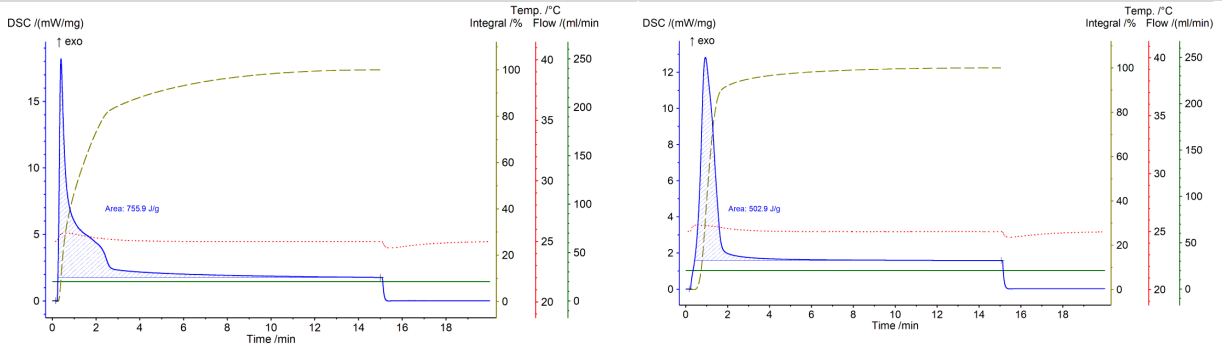

(a) (b)

Figure S79. DSC signal obtained during photo measurements (initiator **7M-P** + OXT-221): (a) under LED@365nm irradiation; (b) under LED@405nm irradiation.

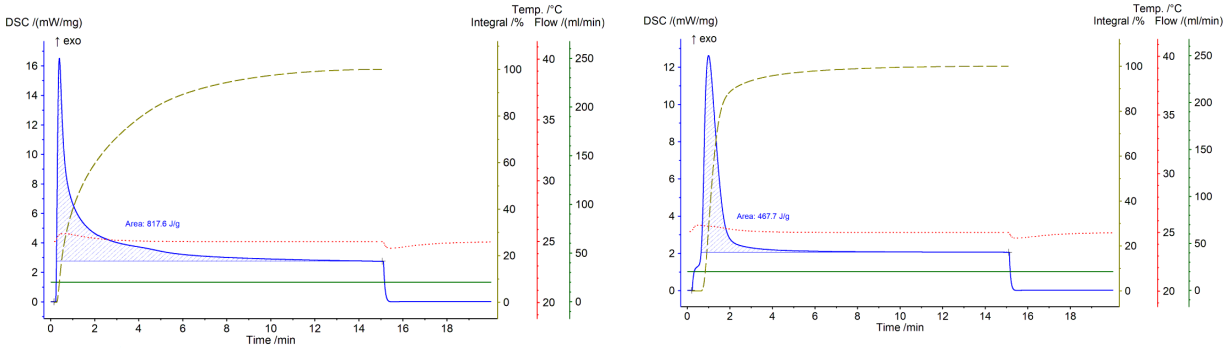

(a) (b)

Figure S80. DSC signal obtained during photo measurements (initiator **7,8M-P** + OXT-221): (a) under LED@365nm irradiation; (b) under LED@405nm irradiation.

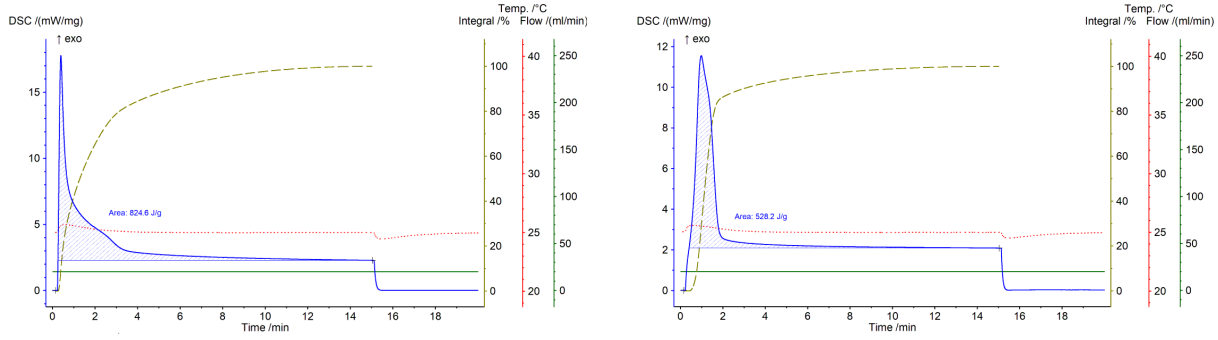

(a) (b)

Figure S81. DSC signal obtained during photo measurements (initiator **7,8ED-P** + OXT-221): (a) under LED@365nm irradiation; (b) under LED@405nm irradiation.

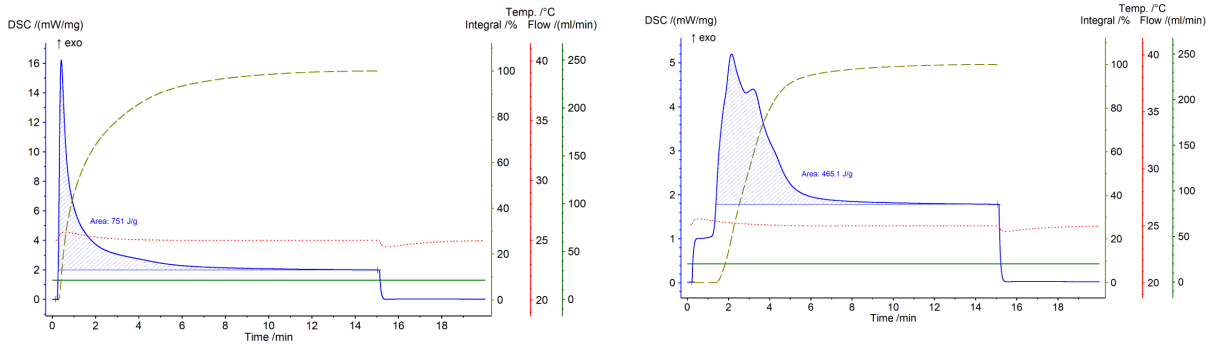

(a) (b)

Figure S82. DSC signal obtained during photo measurements (initiator **7M-8Me-P** + OXT-221): (a) under LED@365nm irradiation; (b) under LED@405nm irradiation.

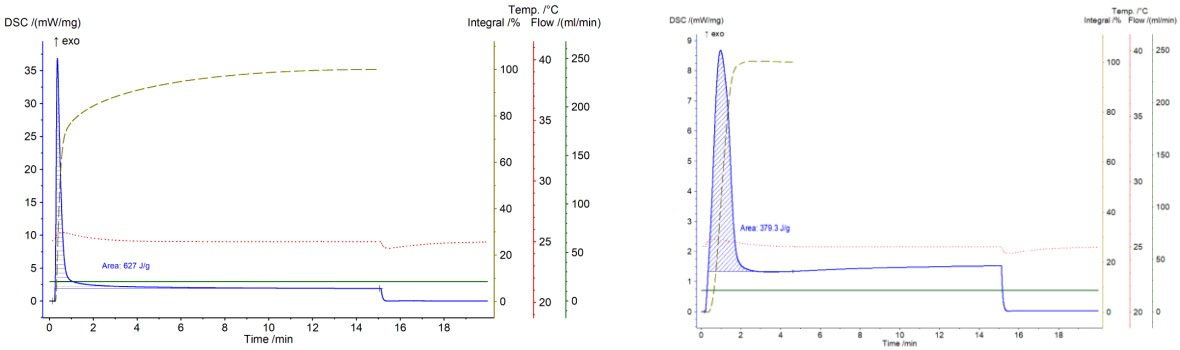

(a) (b)

Figure S83. DSC signal obtained during photo measurements (initiator **5,7M-P** + OXT-221): (a) under LED@365nm irradiation; (b) under LED@405nm irradiation.

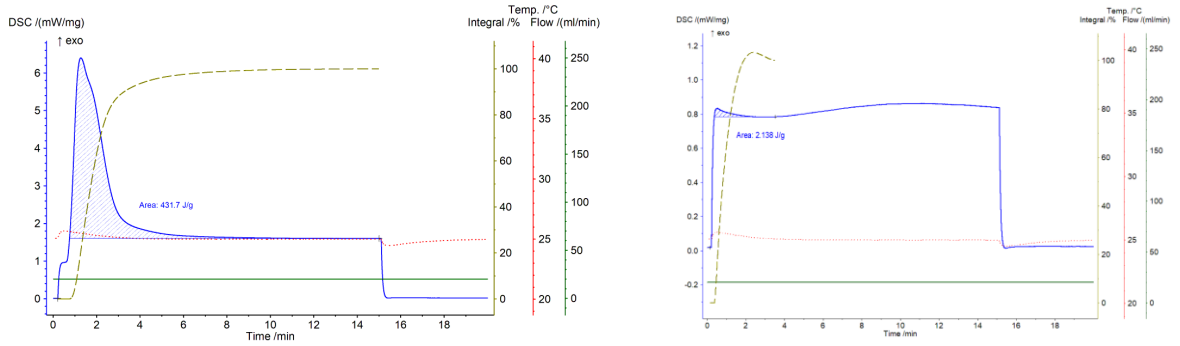

(a) (b)

Figure S84. DSC signal obtained during photo measurements (initiator **5Me-7M-P** + OXT-221): (a) under LED@365nm irradiation; (b) under LED@405nm irradiation.

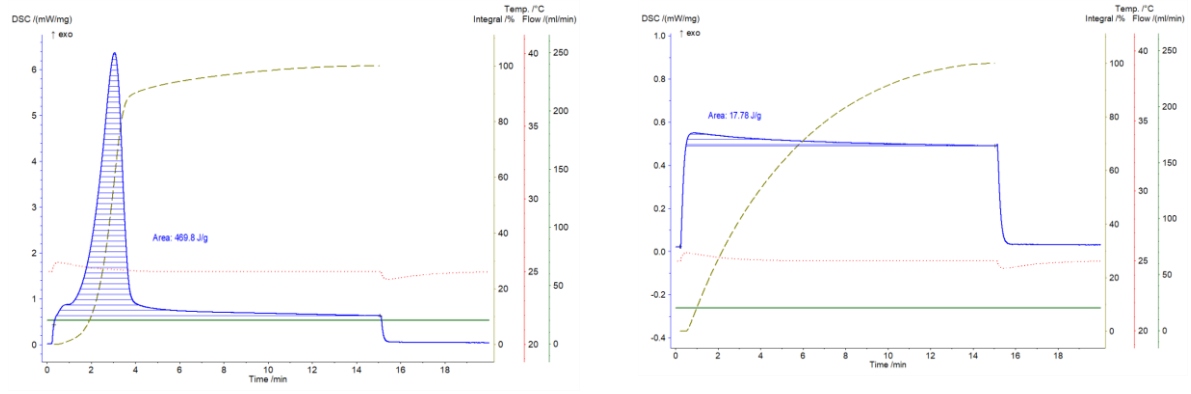

(a) (b)

Figure S85. DSC signal obtained during photo measurements (initiator **IOD** + OXT-221): (a) under LED@365nm irradiation; (b) under LED@405nm irradiation.

Photo-DSC measurements of cationic oxetane resins

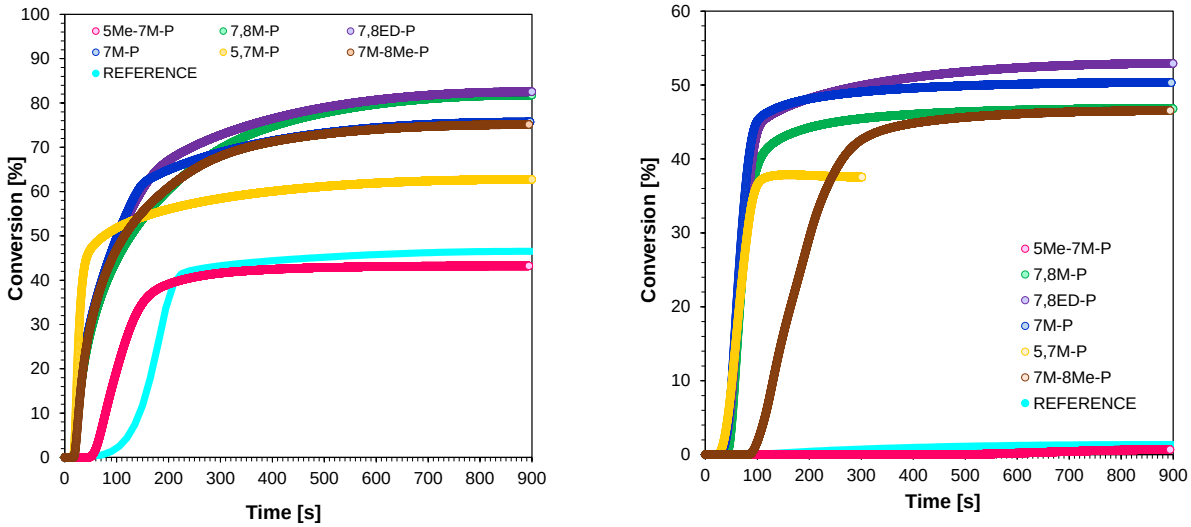

(a) (b)

Figure S86. Conversion profiles for photopolymerization for iodonium photoinitiators in oxetane monomer OXT-221: (a) under LED@365nm irradiation; (b) under LED@405nm irradiation.

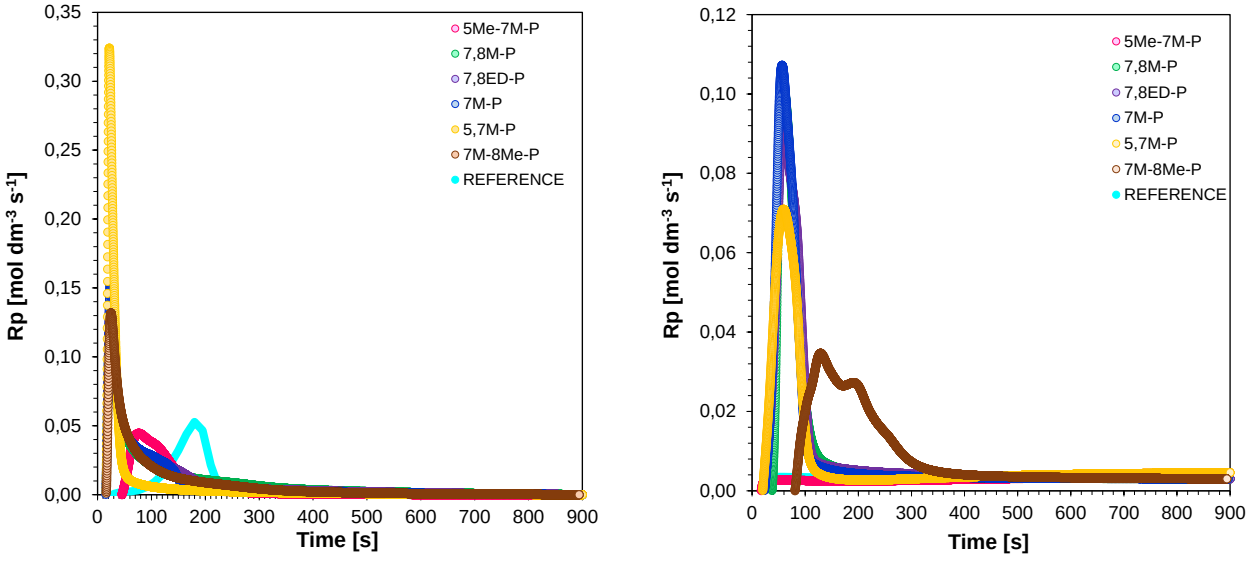

(a) (b)

Figure S87. Rate of photopolymerization for iodonium photoinitiators in oxetane monomer OXT-221: (a) under LED@365nm irradiation; (b) under LED@405nm irradiation.

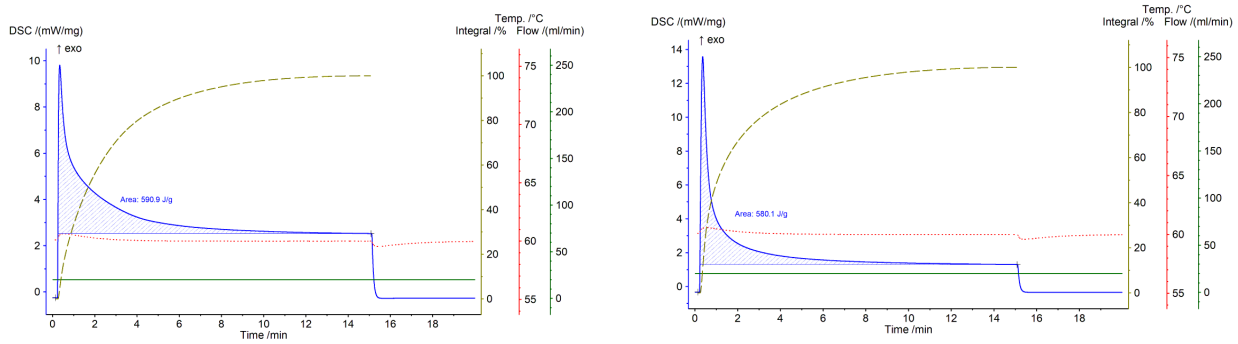

(a) (b)

Figure S88. DSC signal obtained during photo measurements (initiator **7M-P** + BADGE): (a) under LED@365nm irradiation; (b) under LED@405nm irradiation.

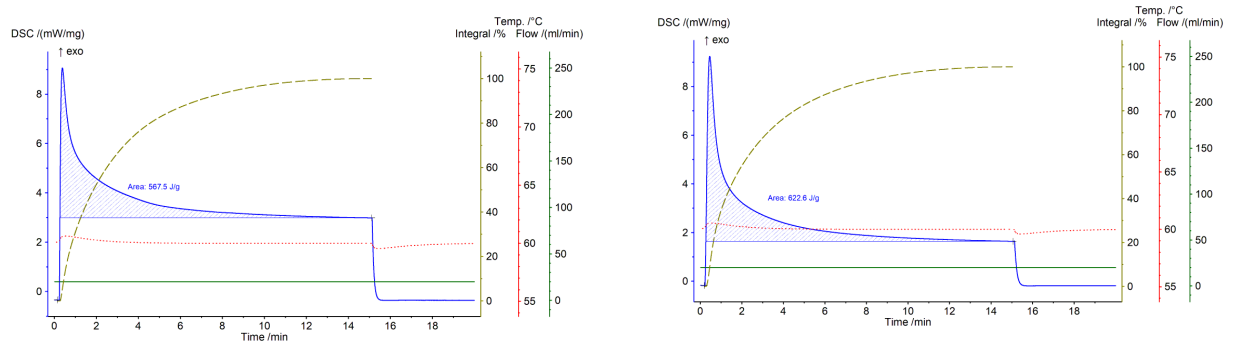

(a) (b)

Figure S89. DSC signal obtained during photo measurements (initiator **7,8M-P** + BADGE): (a) under LED@365nm irradiation; (b) under LED@405nm irradiation.

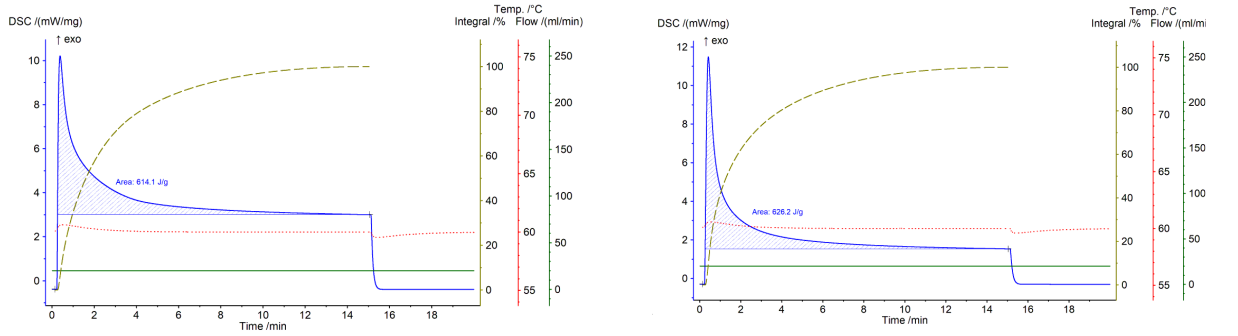

(a) (b)

Figure S90. DSC signal obtained during photo measurements (initiator **7,8ED-P** + BADGE): (a) under LED@365nm irradiation; (b) under LED@405nm irradiation.

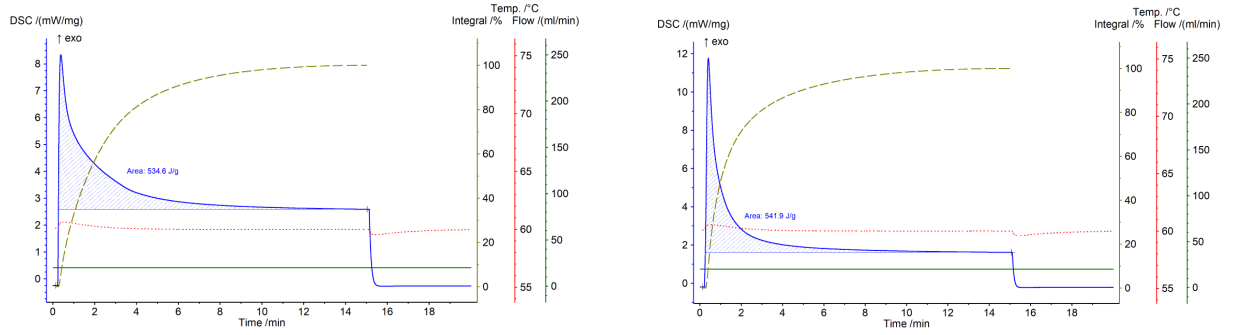

(a) (b)

Figure S91. DSC signal obtained during photo measurements (initiator **7M-8Me-P** + BADGE): (a) under LED@365nm irradiation; (b) under LED@405nm irradiation.

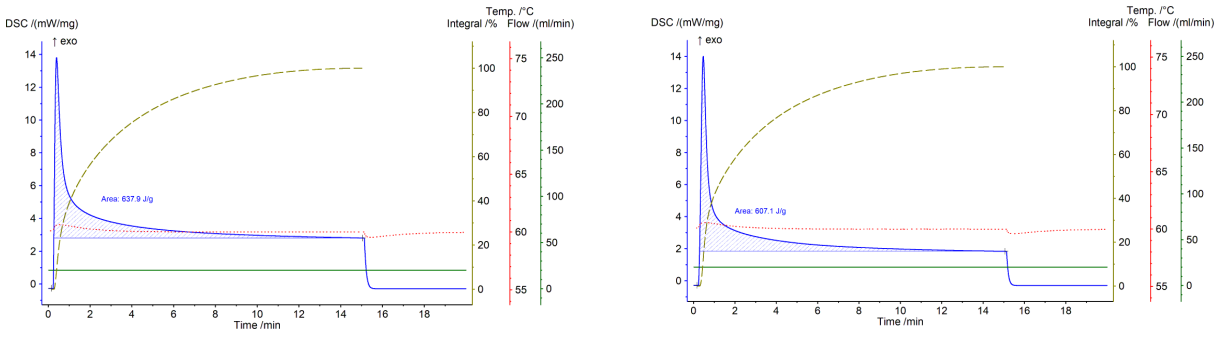

(a) (b)

Figure S92. DSC signal obtained during photo measurements (initiator **5,7M-P** + BADGE): (a) under LED@365nm irradiation; (b) under LED@405nm irradiation.

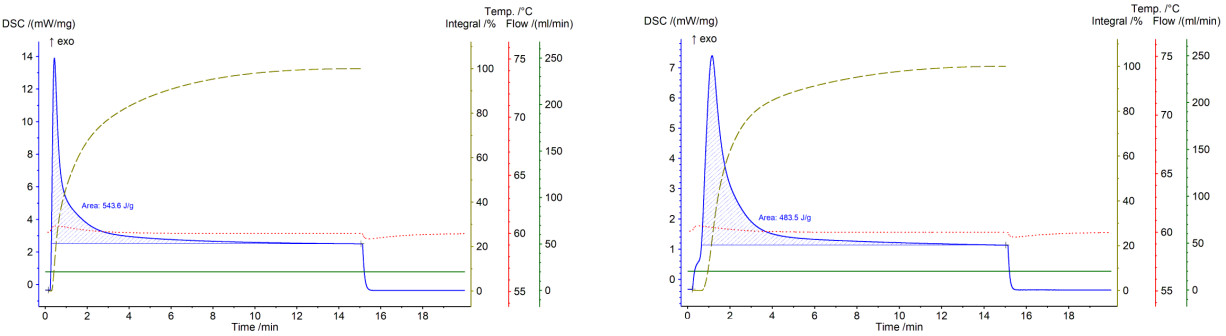

(a) (b)

Figure S93. DSC signal obtained during photo measurements (initiator **5Me-7M-P** + BADGE): (a) under LED@365nm irradiation; (b) under LED@405nm irradiation.

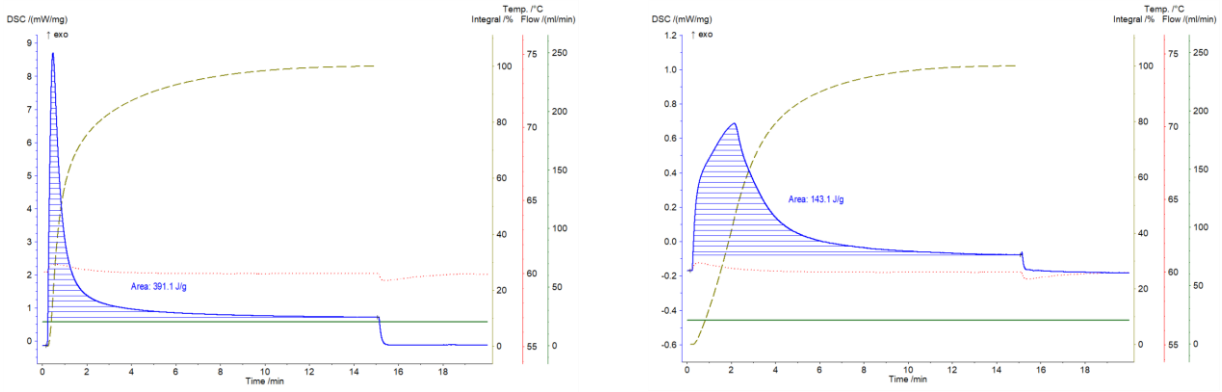

(a) (b)

Figure S94. DSC signal obtained during photo measurements (initiator **IOD** + BADGE): (a) under LED@365nm irradiation; (b) under LED@405nm irradiation.

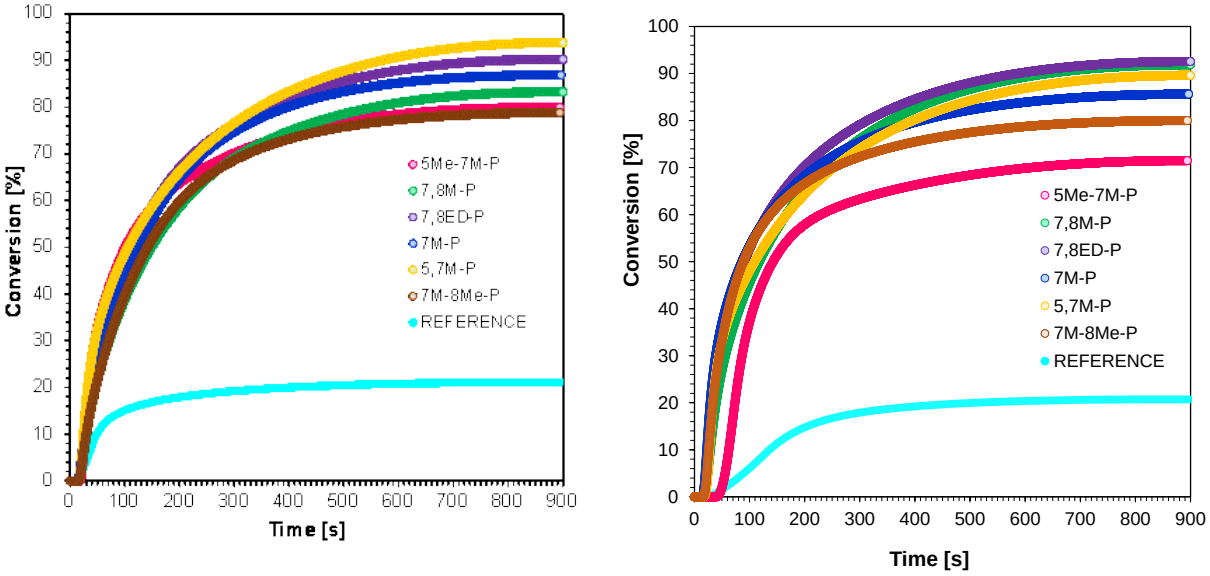

Figure S95. Conversion profiles for photopolymerization for iodonium photoinitiators in glycidyl monomer BADGE: (a) under LED@365nm irradiation; (b) under LED@405nm irradiation.

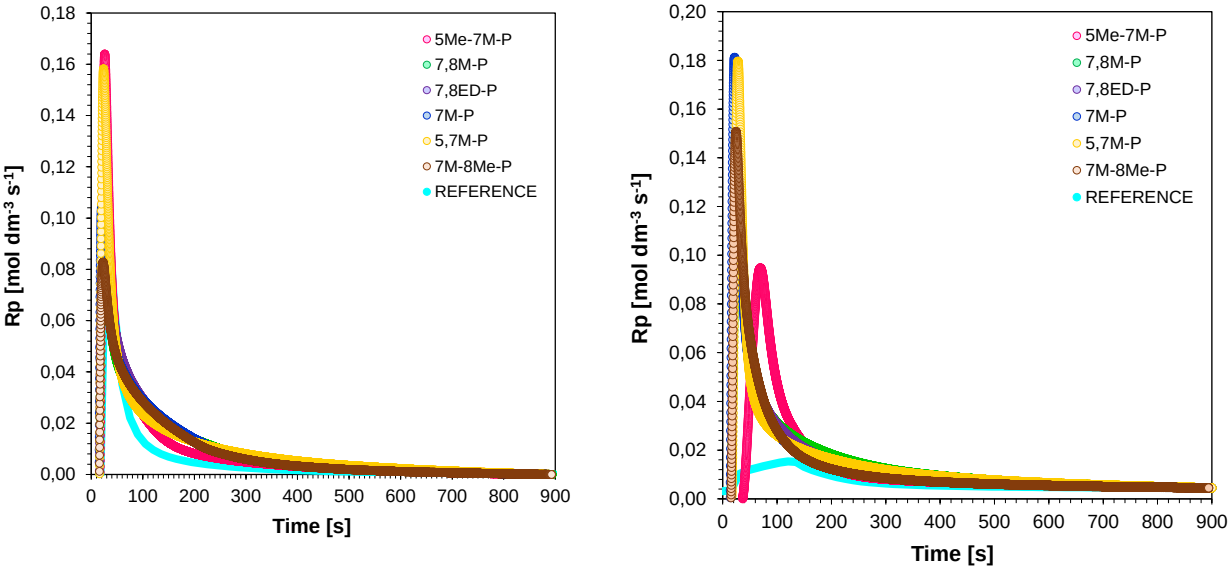

Figure S96. Rate of photopolymerization for iodonium photoinitiators in glycidyl monomer BADGE: (a) under LED@365nm irradiation; (b) under LED@405nm irradiation.

8. Investigating the kinetics of photopolymerization of resins that have found application in 3D printing

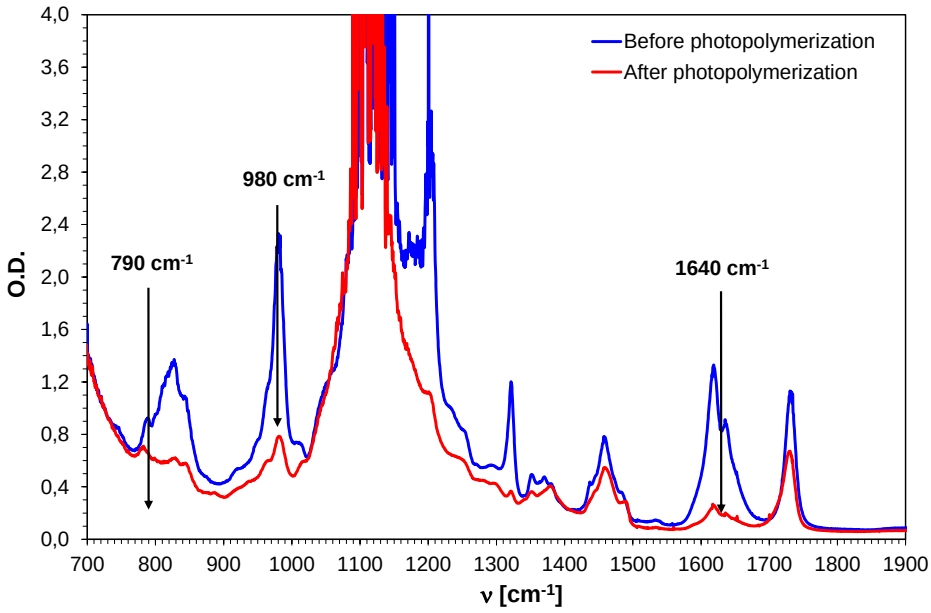

Figure S97. Spectra before and after photopolymerization of epoxy, oxetane and vinyl monomers with initiator **7M-P** under LED@405nm irradiation.

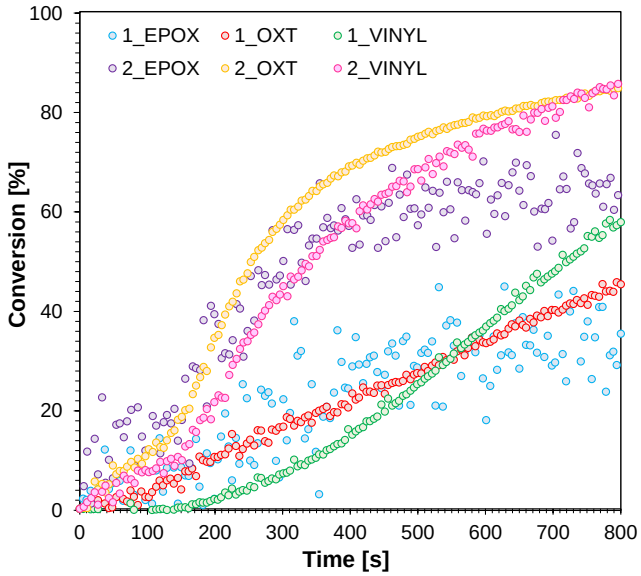

Figure S98. Kinetic profiles obtained during the cationic hybrid photopolymerization of epoxy, oxetane and vinyl monomers for one component photoinitiating systems based on studied iodonium compounds; radiation source - a diode emitting radiation at a wavelength of 405 nm. (1) 2% 7M-P and CADE/OXT-221/TEGDVE (4/3/3 w/w/w); (2) 2% 7M-P and NANOPOX A 611/OXT-221/TEGDVE (4/3/3 w/w/w)

Table S2. Monomers final conversion of resins 1 and 2 used in 3D-VAT printing experiment.

Resin	Conversion [%]	Maximum monitored bandwidth
1	58	VINYL at 1640 cm^{-1}
	30	EPOX at 790 cm^{-1}
	45	OXT at 980 cm^{-1}
2	86	VINYL at 1640 cm^{-1}
	56	EPOX at 790 cm^{-1}
	85	OXT at 980 cm^{-1}

Table S3. Determined printing parameters for resin 1 and 2 and 3D-VAT printing conditions.

3D printing parameters			
Resin	**Equation**	**Critical energy (E_c) [mJ/cm^2]**	**Light penetration depth (D_p) [µm]**
1	y=684.13ln(x)-3588.20	189.60	693.68
2	y=535.09ln(x)-2860.50	209.73	529.05
(1) 2% 7M-P and CADE/OXT-221/TEGDVE (4/3/3 w/w/w) (2) 2% 7M-P and NANOPOX A 611/OXT-221/TEGDVE (4/3/3 w/w/w)			

3D printing process conditions					
Resin	**Exposure time for lower layers [s]**	**Exposure time [s]**	**Light intensity [mW/cm^2]**	**Power [%]**	**Layer thickness [µm]**
1	150	30	9.95	100	100
2					

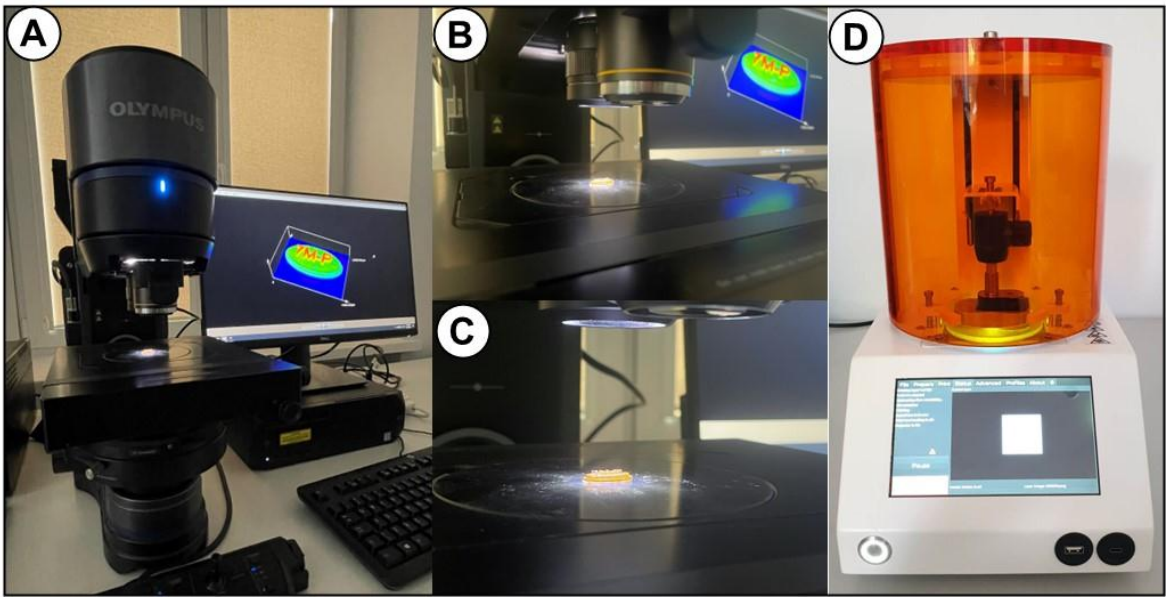

Figure S99. Equipment for 3D-VAT printing and analyzation of printouts: A, B, C - OLYMPUS DSX1000 optical microscope, D - Lumen X+™ 3D printer.

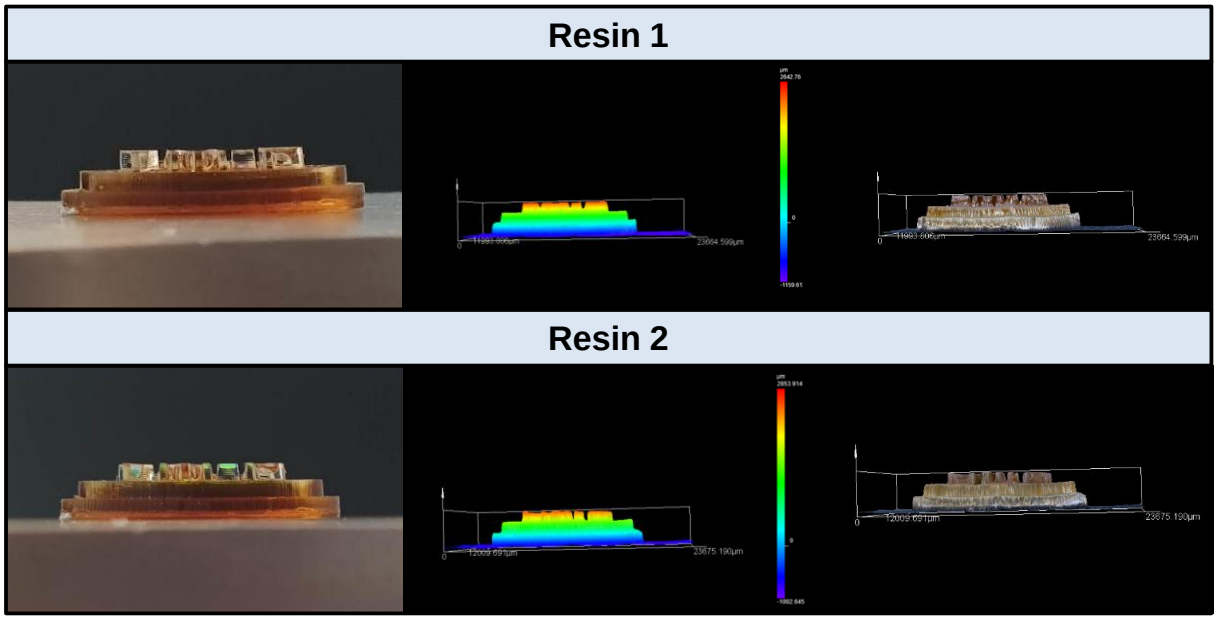

Figure S100. Photographs of prints obtained from resin 1 and 2. Respectively from upper left to right: images of free standing prints, maps of the height, images of prints on the basis of which the maps were prepared.

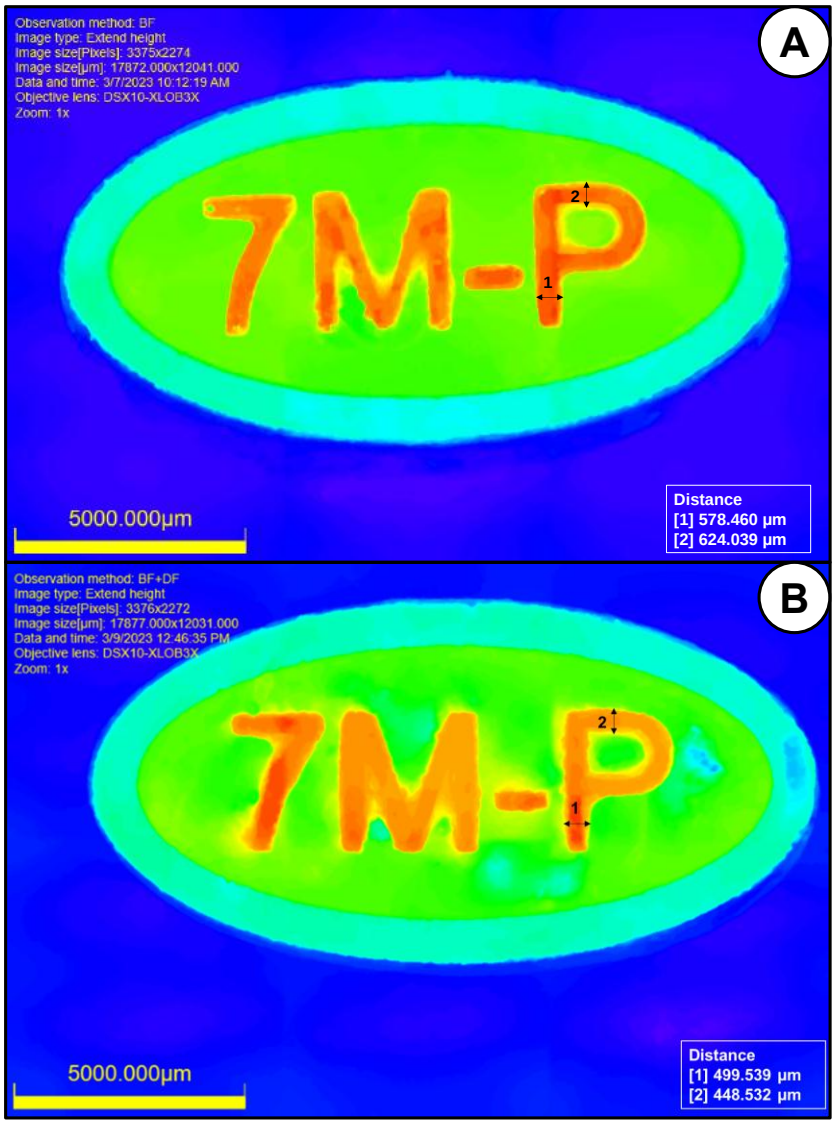

Figure S101. The comparison of resolution for prints obtained from resin 1 (A) and resin 2 (B).